HYDROLOGICAL PROCESSES
Hydrol. Process. (2016)
Published online in Wiley Online Library
(wileyonlinelibrary.com) DOI: 10.1002/hyp.10840

Particulate carbon and nitrogen dynamics in a headwater catchment in Northern Thailand: hysteresis, high yields, and hot spots

Alan D. Ziegler,[1]* Shawn G. Benner,[2] Melvin L. Kunkel,[2] Valerie X.H. Phang,[1] Massimo Lupascu[1] and Chatchai Tantasirin[3]

[1] *Geography Department, National University of Singapore, Singapore*
[2] *Department of Geosciences, Boise State University, Boise, ID, 83702, USA*
[3] *Faculty of Forestry, Kasetsart University, Bangkok, Thailand*

Abstract:

Rivers of South and Southeast Asia disgorge large suspended sediment loads, reflecting exceptionally high rates of erosion promoted by natural processes (tectonic and climatic) and anthropogenic (land-use change) activities that are characteristic of the region. While particulate carbon and nitrogen fluxes have been characterized in some large Asian rivers, less is known about the headwater systems where much sediment and organic material are initially mobilized. This study, conducted in the 74-km^2 Mae Sa Experimental Catchment in northern Thailand, shows that the Sa River is an important source for particulate organic carbon (POC) and particulate organic nitrogen (PON) transported to larger river systems and downstream reservoirs. However, the yields during three years of investigation varied greatly: 5.0–22.3 Mg POC km^{-2} y^{-1} and 0.48–2.02 Mg PON km^{-2} y^{-1}. The 22.3 Mg POC km^{-2} y^{-1} yield is the highest reported for any river on the Asian continent. Stream samples collected during 12 storms showed that almost 3% of the total suspended solid load is POC 0.7 μm to 2.0 mm in size. This percentage is higher than other values for most large rivers on the continent. Further, we documented a strong pulse hysteretic behaviour in the stream, whereby peak fluxes of POC and PON are often delayed (anticlockwise hysteresis) or accelerated (clockwise hysteresis) relative to stream flow peaks (or are complex), complicating the prediction of storm-based or annual particulate carbon and nitrogen fluxes. Stream turbidity and total suspended sediment are reasonable proxies for POC and PON concentrations, while stream discharge is not a good predictor variable. Observed C:N ratios for measured particulate samples range from 3 to 83, with the high-end values likely associated with fresh (non-decomposed) vegetative material greater than 2 mm in diameter. The C:N ratio (weighted based on three sediment sizes) for 12 events ranges from 7.5 to 15.3. These modest values reflect the relatively low C:N ratios for small size fractions (0.7–0.63 μm) that comprise 50–90% of the TSS load in the events. Overall, organic material <0.63 μm contribute about 75% of the total POC load and 80% of the PON load. The annual C:N ratio for the river is approximately 10–11. Collectively, our findings indicate the occasionally high yields make the Sa River—and potentially other similar headwater rivers—a hot spot for POC and PON transported to downstream water bodies. Complex hysteresis patterns and high year-to-year variability hinders our ability to calculate and predict these yields without continuous, automated monitoring of discharge and turbidity. Copyright © 2016 John Wiley & Sons, Ltd.

KEY WORDS carbon; nitrogen; hysteresis; sediment transport; SE Asia; turbidity; C:N ratio

Received 19 November 2013; Accepted 2 March 2016

INTRODUCTION

Global riverine transport of total suspended solids (TSS) to the ocean is an estimated 13–19 Pg y^{-1}, indicating high rates of natural and anthropogenic erosion (Milliman and Meade, 1983; Beusen *et al*., 2005). Particulate organic carbon (POC) and particulate organic nitrogen (PON) are components of TSS that are important in understanding global biogeochemical cycles and water quality in coastal areas (Beusen *et al*., 2005). Total global riverine carbon (C) and nitrogen (N) fluxes to the ocean are estimated at 0.20–1.33 Pg C y^{-1} and 0.03 Pg N y^{-1}, respectively (Ludwig *et al*., 1998, Ittekkot and Zhang, 1989; Beusen *et al*., 2005). Changes in the flux of riverine POC through the loss of previously sequestered soil carbon can negatively alter the terrestrial carbon balance (Meybeck, 1993, Ludwig *et al*., 1996; Mackenzie *et al*., 1998; Jickells, 1998; Schlunz and Schneider, 2000; Lal, 2003; Seitzinger *et al*., 2005; Huang *et al*., 2012). The flux of POC also influences downstream degassing of carbon dioxide (Richey *et al*., 2002). Significant increases in fluvial PON may signal unsustainable land-cover/land-

*Correspondence to: Alan D. Ziegler, Geography Department, National University of Singapore, Singapore.
E-mail: adz@nus.edu.sg

use changes and other anthropogenic activities that accelerate erosion rates and disturb soil quality (Ittekkot and Zhang, 1989; Pimentel *et al*., 1995; Smil, 1999; Gruber and Galloway, 2008).

The Asia and Oceania regions experience high erosion rates and equally high rates of particulate carbon and nitrogen fluxes to the oceans (Gupta, 1996; Ludwig *et al*., 1996; Lyons *et al*., 2002; Meybeck *et al*., 2003; Beusen *et al*., 2005; Coynel *et al*., 2005; Seitzinger *et al*., 2005). An estimated 24% (0.13 of 0.53 Pg) of the total carbon delivered to the oceans by South and Southeast Asian rivers is POC (Huang *et al*., 2012). The occurrence of high POC yields in the two regions is in part tightly coupled with high sediment yields that are attributed to the convergence of active tectonics producing high relief and high precipitation, particularly on some island nations (Ahnert, 1970; Summerfield and Hulton, 1994; Finlayson *et al*., 2002; Dadson *et al*., 2003). For example, some islands of Taiwan have reported POC yields >20 Mg C km^{-2} y^{-1} (Table I). Exceptionally high yields ranging from 102–238 Mg C km^{-2} y^{-1} have been reported for Timor and rivers in New Zealand, having TSS yields $>10\,000$ Mg km^{-2} y^{-1} (Table I). In comparison, POC yields >10 Mg C km^{-2} y^{-1} have been determined for only a few rivers in continental Asia, including the Irrawaddy and Salween Rivers of Myanmar (Robinson *et al*., 2007; Bird *et al*., 2008; Table I).

Only a handful of PON estimates are available for Asian river systems, including the Lanyang-Hsi River in Taiwan (Kao and Liu, 1996, 2000; Liu *et al*., 2008a, b), the Sepik River in Papua New Guinea (Kineke *et al*., 2000; Burns *et al*., 2008), the Longchuanjiang River in China (Lu *et al*., 2011; 2012), the Brantas River in Java of Indonesia (Aldrian *et al*., 2008), and several catchments on Timor (Alongi *et al*., 2013). The highest measured PON values are for river systems in Timor (49 Mg N km^{-2} y^{-1}). For individual rivers, the Lanyang-Hsi River in Taiwan has the highest reported PON yield (4.7 Mg N km^{-2} y^{-1}; Table I). The PON yields determined for the Brantas, Sepik, and Longchuanjiang Rivers are 3.0, 1.7, and 0.24 Mg N km^{-2} y^{-1}, respectively (Burns *et al*., 2008; Lu *et al*., 2011). The modeling study of Beusen *et al*. (2005) estimated PON values ranging from 0.2 to 1.6 Mg N km^{-2} y^{-1} for the Fly (PNG), Salween (Myanmar), Irrawaddy (Myanmar), Ganges/Brahmaputra (India/Bangladesh), Yangtze (China), and Godavari (India) Rivers (Table I). Data available for other selected rivers in the world have a similarly low range of values (0.03–1.7 Mg N km^{-2} y^{-1}; Table I).

The wide range of POC and PON values for just a handful of rivers in this part of the world reinforces the importance of conducting new studies to better understand the fluxes and mechanisms underlying the large reported variations. In some instances, high yields may be natural (Alin *et al*., 2008; Hilton *et al*., 2010; Hung *et al*., 2012), but in others they could be attributed to accelerated erosion and land degradation (Kao, 1996; Lyons *et al*., 2002; Lu *et al*., 2012). Throughout much of the region, road building, logging, land-cover conversion, and intensification of agriculture have been found to accelerate erosion, leading to a subsequent loss of soil carbon and nitrogen (Lal, 2003; Jennerjahn *et al*., 2008; Atapattu and Kodituwakku, 2009; Bruun *et al*., 2009; Ziegler *et al*., 2009; Sidle and Ziegler, 2012). Arguably, insufficient research has been conducted in small headwater catchments where these activities are taking place (Douglas, 1996; Sidle and Ziegler, 2012).

In this study, we document the dynamics and catchment yields of POC and PON in the headwater Sa River in northern Thailand. The upper range of total suspended solid yields in the catchment (839 Mg km^{-2} y^{-1}, Table II) is among the highest reported for the South Asia continent (Ziegler *et al*., 2014b). Interestingly, the total suspended solid yield in the catchment is nearly 10-fold higher than that reported for the upper Chao Phraya River, for which the Sa River is a headwater (Alford, 1992). This relationship suggests that the Sa River is a disproportionately large sediment source to downstream water bodies—and therefore, it may also be a disproportionately large source of POC and PON within the greater Chao Phraya River system.

STUDY SITE

The Mae ('river' in Thai language) Sa Experimental Catchment (MSEC), a headwater catchment of the Ping River, is located northwest of Chiang Mai city in northern Thailand (18°54'06.8″; 98°53′14.2″; Figure 1). The 74.2-km^2 catchment is mountainous, with elevations ranging from 500 to 1400 m asl. The topography is characterized by steep slopes and narrow valleys. The geology of the watershed includes granites and gneiss with some marble and limestone. Soils include Ultisols, Alfisols, and Inceptisols (FAO, 2014). Land cover is primarily mixed secondary forests and scrublands (together approx. 80%), with ongoing conversion to agriculture, especially tree crops, floriculture, and greenhouse operations taking place. These agricultural activities, in addition to ecotourism, support the economies of several small villages. Much of the development, including the building and maintenance of major roads, is located immediately adjacent to the Sa River and its tributaries.

The catchment is the site of ongoing investigations of hydrological and land-use change (Sidle and Ziegler, 2010; Bannwarth *et al*., 2014a, b; Ziegler *et al*., 2014a, b). Associated instrumentation includes 11 spatially-distributed

Table I. Comparison of total discharge (Q), total suspended solid yields (TSS_{yield}), particulate organic carbon yields (POC_{yield}), and particulate organic nitrogen yields (PON_{yield}) for several rivers in the region and elsewhere

River/catchment	Area (km^2)	Q ($10^9\ m^3\ y^{-1}$)	TSS_{yield} ($Mg\ km^{-2}\ y^{-1}$)	POC_{yield} ($Mg\ km^{-2}\ y^{-1}$)	PON_{yield} ($Mg\ km^{-2}\ y^{-1}$)	POC/TSS** (—)	C:N***	Reference
Islands (Oceania and Asia)								
Timor catchments	5040	170	11 706	238	49	0.020	4.9	Alongi *et al.* (2013)
Hikuwai (NZ)	307–550	0.27–0.58	13 890–14 200	222	—	0.016	—	Lyons *et al.* (2002; 2005); Hicks *et al.* (2004)
Haast (NZ)	1020	6.63	4500–12 700	15–168	—	0.011	8–13	Hilton *et al.* (2008) based on Lyons *et al.* (2005); Lyons *et al.* (2002).
Waiapu (NZ)	1378–1734	2.7	17 800	115	—	0.006	—	Hicks *et al.* (2004), Thompson (2009)
Whataroa (NZ)	453	—	10 325	102	—	0.010	12–23	Hilton *et al.* (2008), TSS based on Lyons *et al.* (2005)
Poerua (NZ)	136	—	26 200	91	—	0.003	13–19	Hilton *et al.* (2008), TSS based on Korup *et al.* (2004)
Waitangitaona (NZ)	72	—	12 500	83	—	0.007	12–20	Hilton *et al.* (2008), TSS based on Korup *et al.* (2004);
Mangatu (NZ)	183	0.23	11 540–12 076	72.1	—	0.006	—	Hicks *et al.* (2000); Gomez *et al.* (2003)
Gaoping (Taiwan)	3257	8.5	3600	69.2	—	0.019	5–8	Hung *et al.* (2012); Hilton *et al.* (2010); Liu *et al.* (2009)
Wanganui (NZ)	344	—	12 500	56	—	0.004	12–16	Hilton *et al.* (2008)
Waipaoa (NZ)	1580	1.07	6640	54.9	—	0.008	—	Hicks *et al.* (2004)
Cropp (NZ)	29	0.29	30 000–32 120	52	—	0.002	—	Lyons *et al.* (2002; 2005)
Hokitika (NZ)	307–352	3.31	6313–17 000	43–47	—	0.002	13–18	Lyons *et al.* (2002); Hilton *et al.* (2008), TSS based on Lyons *et al.* (2005)
Fly (PNG)	18 400	98	3804	38	1.6*	0.100	7.8	Alin *et al.* (2008)
Fox (NZ)	92	—	12 500	37	—	0.003	10.5	Hilton *et al.* (2008)
Waiho (NZ)	164	—	10 325	27	—	0.003	9–10	Hilton *et al.* (2008)
Lanyang-Hsi (Taiwan)	820	1.81	8335	23	4.7	0.002		Kao and Liu (1996; 2000); Liu *et al.* (2008a, b)
Sepik (PNG)	77 000	160	1104	17.1	1.70	0.016	10.1	Burns *et al.* (2008); Kineke *et al.* (2000)
Strickland (PNG)	36 740	71	833	13	—	0.016	10–16	Alin *et al.* (2008)
Sebangau (Kalimantan, Indonesia)	5200	14.41	—	5.8	—	—	—	Moore *et al.* (2011)
Brantas (Java, Indonesia)	11 050	18.9	272	4.29	3	0.016	—	Aldrian *et al.* (2008)
Waikato (NZ)	12 000	10.06	12	1.13	—	0.094	—	Ludwig *et al.* (1996)
Thompson Creek (Australia)	1.7	0.001	—	0.48	—	—	15–30	Bass *et al.* (2011)
Wanquan (Hainan, China)	3693	5.2	1083	0.68	—	0.001	4–10	Wu *et al.* (2012)
Continental Asia								
Mae Sa (Thailand)	74.16	0.03–0.06	160–839	5.0–22.3	0.48–2.02	0.028	10–11	This study
Salween (Myanmar)	271 914	211	188–206	8.8–12.5	0.3*	0.054	9–14	Bird *et al.* (2008); Robinson *et al.* (2007)
Irrawaddy (Myanmar)	413 710	697	265–365	5.3–10.4	0.9*	0.025	6–10	Bird *et al.* (2008); Robinson *et al.* (2007)
Indravati (India)	41 665	32.85	—	7.13	—	—	—	Balakrishna and Probst (2005)

Continues

Table I. (Continued)

River/catchment	Area (km^2)	Q (10^9 m^3 y^{-1})	TSS_{yield} (Mg km^{-2} y^{-1})	POC_{yield} (Mg km^{-2} y^{-1})	PON_{yield} (Mg km^{-2} y^{-1})	POC/TSS** (—)	C:N***	Reference
Sungai Gombak (Malaysia, cleared)	103	0.13081	—	6.16	—	—	—	Bishop (1973) in Schlesinger and Melack (1981)
Pranhita (India)	109 077	36.81	—	5.68	—	—	—	Balakrishna and Probst (2005)
Brahmaputra /Brahmaputra (India/Bangladesh)	1 600 000	1000	588–670	3.75–5.22	0.5–0.8*	0.007	—	Ludwig *et al.* (1996); Capone *et al.* (2008); Aucour *et al.* (2006)
Longchuanjiang (China)	1800	0.34	150	4	0.24	0.027	7.27	Lu *et al.* (2011; 2012)
Yangtze (China)	1 800 000	990–995	250–267	1.2–3.3	0.2*	0.009	—	Wu *et al.* (2007); Ni *et al.* (2008); Beusen *et al.* (2005)
Sungai Gombak (Malaysia, forested)	28	0.03556	—	2.44	—	—	—	Bishop (1973) in Schlesinger and Melack (1981)
Godavari (India)	313 000	89–105	543	2.2–2.4	0.2*	0.004	12	Sarin *et al.* (2002); Balakrishna and Probst (2005); Panda *et al.* (2011)
Wardha (India)	47 982	11.91	—	3.06	—	—	—	Balakrishna and Probst (2005)
Mekong (Cambodia)	795 000	475	96	2.1	—	0.022	11.11	Ellis *et al.* (2012)
Sabari (India)	24 042	13.6	—	2.05	—	—	—	Balakrishna and Probst (2005)
Indus (Pakistan)	912 000	100	260	1.79	—	0.007	—	Ludwig *et al.* (1996)
Xijiang (China)	353 000	118	80	1.21	—	0.015	—	Sun *et al.* (2007); also see Wei (2003) and Gao *et al.* (2002)
Pearl (China)	500 000	280	50	1.2	—	0.024	—	Ni *et al.* (2008)
Luodingjiang (China)	3164	2.7	85	1.1	—	0.013	—	Zhang *et al.* (2009)
Zengjiang (China)	2866	3.82	84.7	0.80	—	0.009	9–11	Gao *et al.* (2007)
Pravara (India)	6634	1.4	—	0.63	—	—	—	Balakrishna and Probst (2005)
Yellow (China)	752 000	25.2	256	0.55	1.7	0.002	6	Ran *et al.* (2013); Liu *et al.* (2008); Capone *et al.* 2008
Penganga (India)	23 895	5.11	—	0.24	—	—	—	Balakrishna and Probst (2005)
Purna (India)	15 579	2.83	—	0.17	—	—	—	Balakrishna and Probst (2005)
Manjara (India)	30 844	7.64	—	0.10	—	—	—	Balakrishna and Probst (2005)
Manair (India)	12 313	2.8	—	0.08	—	—	—	Balakrishna and Probst (2005)
Other								
Guaba (PR)	0.114	0.0004	—	27.41	—	—	—	Murphy and Stallard (2012)
Capesterre (Guadeloupe)	16.56	0.048	67–213	8.1–25.5	0.55–1.7	0.120	—	Lloret *et al.* (2012)
Icacos (PR)	3.26	0.01	164–2140	2.0–21.48	0.12–0.22	0.010	—	McDowell and Asbury (1994); Murphy and Stallard (2012)
Cayaguas (PR)	26.4	0.04	2110	19.16	—	0.009	—	Murphy and Stallard (2012)
Canovanas (PR)	25.5	0.03	424	7.53	—	0.018	—	Murphy and Stallard (2012)
Mameyes (PR)	17.8	0.05	325	6.04	—	0.019	—	Murphy and Stallard (2012)
Wailuku (Hawaii, USA)	598–659	0.14–0.26	2.4	0.82–1.78	0.06–0.13	—	—	Wiegner *et al.* (2009)
Sonadora (PR)	2.62	0.006–0.007	16–23	0.64–0.91	0.041–0.055	—	—	McDowell and Asbury (1994)
Toronja (PR)	0.16	0.0002–0.0004	19–33	0.41–0.9	0.032–0.067	—	—	McDowell and Asbury (1994)

*Model result of Beusen *et al.* (2005).
**Calculated at the midpoint of POC range / midpoint of TSS range.
***Calculated at the midpoint range if not reported.

Table II. Mae Sa Experimental Catchment annual rainfall, runoff, runoff coefficient (ROC = rainfall / runoff), total suspended sediment (TSS) yield, total particulate organic carbon (POC) yield, total particulate nitrogen (PON) yield for 2006–2008

Year		2006	[2006]$^+$	2007	[2007]$^+$	2008	[2008]$^+$
Rainfall*	(mm)	1934	—	1632	—	1663	—
Runoff *	(mm)	795	—	552	—	414	—
ROC*	(-)	0.41	—	0.34	—	0.25	—
TSS yield*	(Mg km^{-2})	839	—	323	—	160	—
POC yield	(Mg C km^{-2})	22.3	[15.9]$^+$	9.2	[8.2]$^+$	5.0	[5.1]$^+$
PON yield	(Mg N km^{-2})	2.02	[1.50]$^+$	0.84	[0.77]$^+$	0.48	[0.48]$^+$
POC/TSS	(%)	2.7	[1.9]$^+$	2.8	[2.5]$^+$	3.1	[3.2]$^+$
PON/TSS	(%)	0.24	[0.18]$^+$	0.26	[0.24]$^+$	0.30	[0.30]$^+$
POC yield (fine)	(Mg C km^{-2})	15.48	—	6.52	—	3.73	—
POC yield (medium)	(Mg C km^{-2})	6.08	—	2.31	—	1.13	—
POC yield (coarse)	(Mg C km^{-2})	0.73	—	0.32	—	0.19	—
PON yield (fine)	(Mg N km^{-2})	1.62	—	0.69	—	0.40	—
PON yield (medium)	(Mg N km^{-2})	0.37	—	0.14	—	0.07	—
PON yield (coarse)	(Mg N km^{-2})	0.03	—	0.01	—	0.01	—
POC/PON (fine)	—	9.56	—	9.42	—	9.23	—
POC/PON (medium)	—	16.39	—	16.72	—	17.27	—
POC/PON (coarse)	—	26.14	—	24.04	—	23.78	—
POC/PON (all sizes)	—	11.03	—	10.85	—	10.58	—

*Values calculated elsewhere (Ziegler *et al*., 2014b).
$^+$ Values in [ ] for each year are based on the relationship with turbidity (Figure 4b,e). The TSS time series used in the calculation are from Ziegler *et al*. (2014b). All other POC and PON calculations are based on the relationship with TSS (Figure 4c,f). Calculations for all estimates are based on hourly measurements made at the stream gauging station.

rain gages and one river gaging station that continuously monitors discharge and stream water turbidity at the mouth of the catchment on a sub-hourly time scale (Figure 1). Mean annual rainfall of the catchment varies from 1500 to 2000 mm y^{-1}. The vast majority of the annual precipitation is delivered during the monsoon season between May and November. The catchment has a runoff ratio of approximately 30% (Ziegler *et al*., 2014b). Monsoon rain occurs as intense downpours, often exceeding 20 mm h^{-1}. These rain events produce a rapid and dramatic response in streamflow, with the river stage often rising a meter or more within a few minutes (Figure 2). With a wet-season baseflow level of approximately 1.5 m^3 s^{-1}, storm events often produce flow peaks in excess of 10 m^3 s^{-1} in the flashy stream. Storm flow event duration is typically 2–6 h; catchment residence times are typically short in the wet season. This flashy behaviour produces a complex and flashy annual hydrograph (Figure 2).

In a prior work (Ziegler *et al*., 2014b), we found that total annual stream flow was significantly higher in 2006 (795 mm) than in 2007 (552 mm) and 2008 (414 mm) (Table II). Mae Sa total suspended solid concentrations were high during storm events (maximum TSS exceeded 2000 mg l^{-1} for 11 out of 18 monitored events; a maximum of 15 900 mg l^{-1} was recorded). These high suspended sediment concentrations translated into substantial sediment yields: 839, 323, and 160 Mg km^{-2} y^{-1} for the three years, respectively (Table II).

METHODS

Stream sampling was undertaken at the mouth of the Mae Sa catchment (Stream gage station 434, Figure 1). Sampling methods, which are described in detail by Ziegler *et al*. (2014b), are summarized here. Sampling was generally conducted within 2–6 h periods containing the rising limb, peak, and part of the falling limb of the storm hydrograph. Storm duration, ranging from 7 to 24 h (Table III), was determined from the time that the baseflow measurement was taken until the time the hydrograph returned to a new baseflow level (Q responses are shown in Figure 3; Table III). Catchment residence time for most runoff water was short, with flow peaks arriving approximately 1–3 h after the period of maximum precipitation (Figure 3; Ziegler *et al*., 2014b). Discharge was determined based on (1) stage measurements determined from a Campbell (Campbell Scientific, Logan UT, USA) pressure transducer (CS451) and Campbell CR10x data logger at one-minute intervals; and (2) a stage-discharge curve that was developed from 56 stage-velocity measurements (described in Ziegler *et al*. (2014b)).

Automated turbidity measurements were made with an Analyte (Australia) NEP-395 infrared-based turbidity probe, housed in a PVC pipe that was suspended from a walking bridge to allow the probe to freely float 10–20 cm below the water surface (Ziegler *et al*., 2014b). Turbidity was also measured minutely with the data

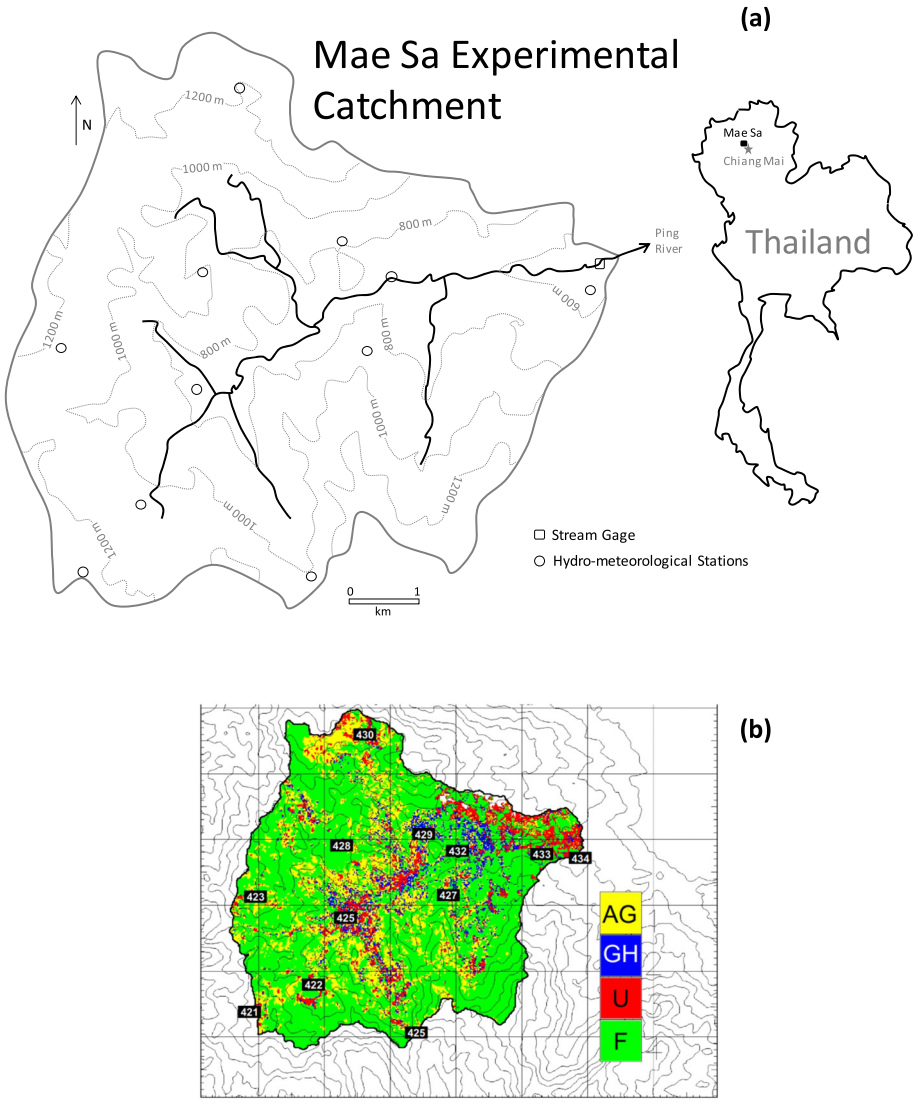

Figure 1. Site map of the Mae Sa experiment site in northern Thailand. Panel (a) shows the watershed location in Thailand, the topography and major stream channels. Panel (b) shows major land covers in the Mae Sa catchment include hill slope and plantation agriculture (AG, 23%), greenhouse agriculture (GH, 7%), urbanized or peri-urban areas (U, 8%), and forest of various degrees of disturbance (F, 62%). Grid cell dimensions are 2 × 2 km. Rectangles demarcate hydro-meteorological measurement sites. Streamflow, total suspended solids, particulate organic carbon, and particulate organic nitrogen measurements were made at the stream gage station 434. Rainfall is measured at all other numbered hydro-meteorological stations (rectangles)

logger. Total suspended solid samples, POC, and PON data were collected using a 20-l bucket from a safe stream-side location during 12 storm events in 2006 and 2007 (Table III, $n = 160$) as well as during a handful of other flow conditions ($n = 21$). Most of the 12 storm events were flashy, with some having multiple peaks (Figure 2 and 3). Rainfall associated with these events ranged from 2.4 to 27.1 mm (Table III). However, these events represent only about 4% of the total rainfall for the two-year period. More details about these storms are reported in Ziegler *et al.* (2014b).

Suspended sediment was separated into coarse (>2000 µm) and medium (63–2000 µm) fractions by wet sieving. The finest fraction (<0.7–63 µm) was separated by subsequently filtering the supernatant of the sieved samples with pre-ashed 0.7-µm Whatman GF/F glass filters. All fractions were oven dried (50 °C) and refrigerated until analysed.

Analysis for total carbon and nitrogen concentration was conducted by dry combustion using a FlashEA® 1112 Elemental Analyzer (Thermo Fisher Scientific, Inc., MA, USA). Analysis standardization was based upon aspartic acid standards; this material was analysed as an internal standard. Laboratory replicates, both between runs and during runs, quantified instrument drift. Organic fractionation was performed by pre-treating samples with two to three drops of concentrated HCl or H_3PO_4 (Soil Survey Staff, 2014). Samples were then air dried in a fume

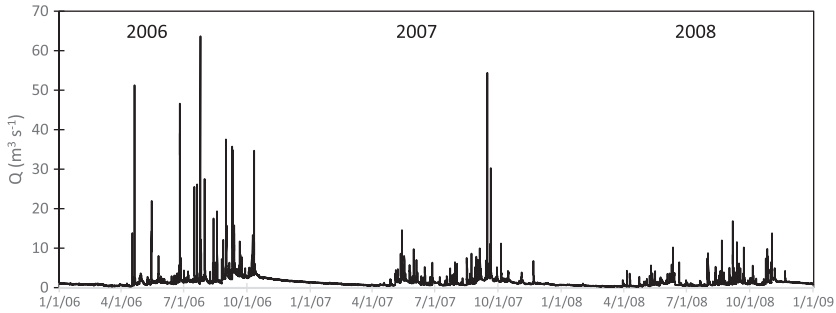

Figure 2. Mae Sa River stream flow hydrograph for 2006–2008 (from Ziegler *et al*., 2014a). Noticeable is the flashness of the stream in response to storm events, the distinct seasonality which is caused by the monsoonal climate, and the difference in high stream flow in 2006 *versus* 2007 and 2008

Table III. Total suspended solid (TSS), particulate organic carbon (POC), and particulate organic nitrogen (PON) during 12 storms

Event	RF	Q	Duration	TSS	POC	PON	POC/TSS	PON/TSS
	mm	mm	(h)	Mg	Mg C	Mg N	—	—
60724	2.5	1.21	20.6	36	1.91	0.22	0.053	0.0061
60728	2.9	0.64	7.0	30	1.39	0.19	0.046	0.0062
60808	8.0	1.52	21.1	92	5.74	0.62	0.062	0.0068
60908	13.5	2.98	23.5	128	5.42	0.36	0.042	0.0028
60909	2.4	1.30	11.5	41	0.93	0.08	0.023	0.0020
60912	24.1	3.03	7.4	579	13.64	0.95	0.024	0.0016
70504	27.1	1.62	13.0	85	3.05	0.25	0.036	0.0030
70614	17.3	1.35	18.8	110	3.03	0.28	0.028	0.0026
70709	6.9	0.51	12.3	11	0.36	0.04	0.033	0.0041
70822	4.5	0.66	7.6	65	1.87	0.23	0.029	0.0036
70823	16.5	2.45	20.9	469	11.31	1.05	0.024	0.0022
70828	16.0	2.25	24.0	204	5.70	0.60	0.028	0.0029

Values for TSS, POC, PON, and C:N are determined from minutely Q and turbidity estimates (see Ziegler *et al*., 2014b for details). The Event ID is the date (year, month, day); RF is rainfall; Q is discharge, Duration is duration on storm for the calculations, C is carbon, and N is nitrogen.

hood until effervescence ceased and then re-dried in an oven at 105 °C. The organic carbon fraction was determined using the FlashEA® 1112 Elemental Analyzer.

Relationships between observed stream flow (Q), turbidity (T), TSS, POC, and PON were evaluated using simple linear regression on log-transformed data. The resulting relationships between variables (described in the Results section) were then used to estimate POC and PON fluxes for 2006, 2007, and 2008. Because particulate carbon and nitrogen are measured discretely and require on-site sampling, estimating annual flux is often based on observed relationships with a continuously measured proxy. In larger river systems, TSS, and by extension POC and PON, are often correlated with stream flow (Coynel *et al*, 2005; Beusen *et al*., 2005; Zhang *et al*., 2009). However, in smaller catchments, such as Mae Sa, the correlation between these variables and stream flow is not strong (section Storm event hysteresis below; Ziegler *et al*., 2014b), necessitating the need for an alternative proxy for estimating annual fluxes. Herein, we use the synthetic hourly TSS times series produced in the previous modeling effort (Ziegler *et al*., 2014b) as well as the measured turbidity time series, which was recorded automatically with Q at the gaging station, to estimate the annual fluxes of POC and PON for three years (2006–2008).

For year-to-year comparisons of various relationships, the non-parametric Mann–Whitney *U*-test (MW-U) was used on untransformed values to test significance at $\alpha = 0.05$.

RESULTS

Stormflow measurements

The median (± one median absolute deviation) discharge, turbidity, and total suspended solids values for all 181 samples were $2.8 \pm 1.4\,m^3\,s^{-1}$, 941 ± 577 NTU, and $1058 \pm 683\,mg\,l^{-1}$, respectively (not shown). The ranges for these variables were large: discharge ($0.8–29.7\,m^3\,s^{-1}$), turbidity (8–3000 NTU), and total suspended solids ($17–9000\,mg\,l^{-1}$). Total suspended solid load ranged from 11 to 579 Mg during the 12 monitored storms (Table III); these loads are discussed in prior work (Ziegler *et al*., 2014b).

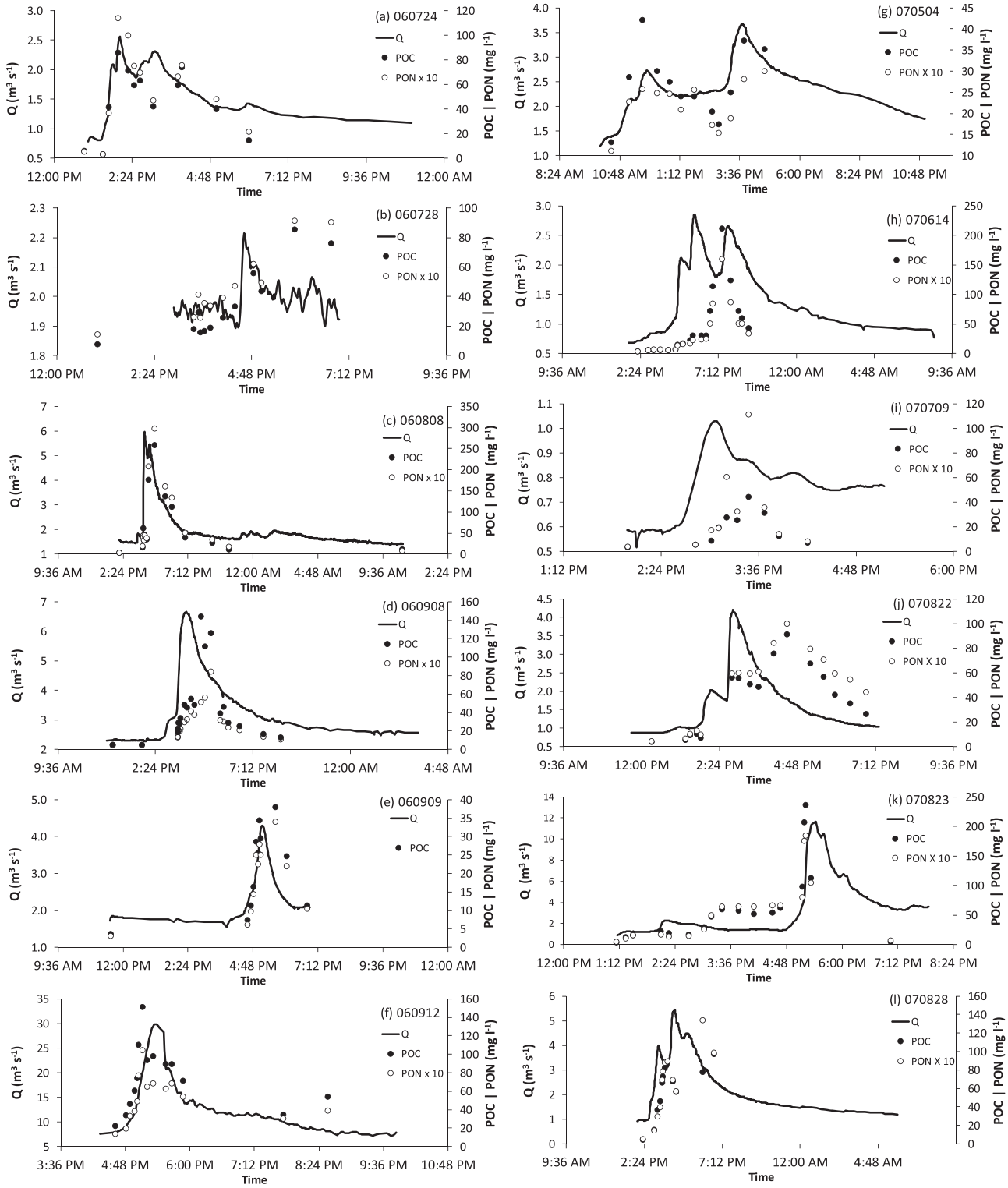

Figure 3. Storm hydrographs showing stream discharge (Q), particulate organic carbon content (POC), and particulate organic nitrogen (PON) during 12 monitored storm events in 2006 and 2007. Note that the PON values are multiplied by a factor of 10 (for viewing). Event IDs refer to year, month, and day

The median POC concentration of all 181 samples was 33.1 ± 21.6 mg C l^{-1}, while median PON was 3.0 ± 2.0 mg N l^{-1} (not shown). The ranges of POC and PON values for the 181 samples were about 2–257 mg C l^{-1} and 0.2–29.7 mg N l^{-1}, respectively. During a storm event, the POC and PON concentrations were at

times asynchronous with changes in discharge, demonstrating a circular pattern relationship or hysteresis effect (discussed in detail below). Total POC loads ranged from 0.36 to 13.64 Mg C and total PON loads ranged from 0.04 to 1.05 Mg N for the 12 storms (Table III).

The POC and PON contributions to storm TSS loads (POC/TSS) ranged from 2.3 to 6.2% (0.023 to 0.062) and 0.2–0.7% (0.0016 to 0.0068), respectively (Table III). The POC/TSS relationship for all three size fractions was not controlled by the total amount of TSS (Figure 4e). However, the relationship for fine- and medium-sized

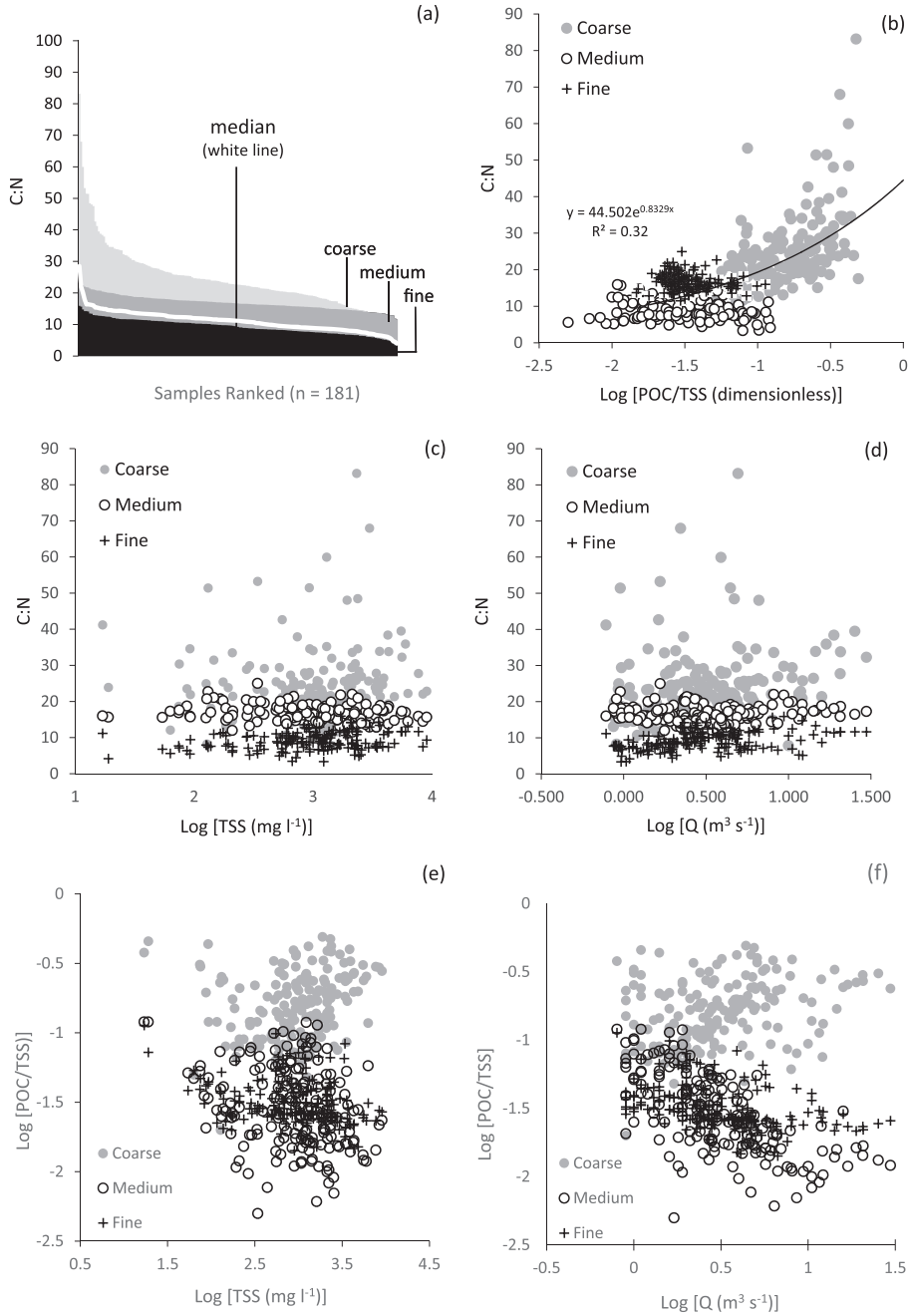

Figure 4. (a) Ranked distribution of C:N values for the 181 particulate organic matter samples collected in this study ($n = 174$ for coarse fraction because some samples did not have material present). Relationships between C:N values for the three size fractions are shown for the following: (b) POC/TSS; (c) TSS; and (d) Q. The relationships between POC/TSS are shown for (e) TSS and (f) Q. The regression equation in panel b pertains only to the coarse fraction; there is no meaningful relationship between C:N and POC/TSS for the fine and medium fractions. In all panels, size fractions are: coarse (>2000 μm), medium (63–2000 μm), and fine (0.7–63 μm); and C is carbon; N is nitrogen; POC is particulate organic carbon; TSS is total suspended solids; and Q is discharge

material was to some extent negatively associated with discharge (log-transformed data). In support, the coefficient of determination (R^2) for regression of the medium fraction with Q as the independent variable was 0.42 (significant at $\alpha = 0.05$; regression line not shown in Figure 4f); the R^2 for fine material and Q was only 0.18 (not shown).

For all events, the fine fraction (0.7–63 μm) comprised more than half (54 to 95%) of the POC material transported (Table 6). Similarly, 58 to 98% of the PON transported during the storms was in the fine fraction (Table IV). The medium fractions of POC and PON comprised 3–40% and 1–31% of their respective total POC and PON loads during the 12 storms (Table IV). The coarse fractions were only 1–9% and 0.2–4%, for POC and PON, respectively. For TSS, the fine fraction comprised 36–95% of the material transported during the 12 events; the contributions of medium (3–52%) and coarse (0.3–1.3%) material were lower (Table IV).

During the 12 events, POC contributed more to coarse TSS loads (8–24%) than to fine (2–7%) or medium (2–8%) loads (Table V). This dominance of the coarse fraction was true for PON for 10 of 12 events (Table V): coarse load (0.35–1.01%); medium load (0.09–0.54%); and fine load (0.20–0.83%). These associations are attributable to the relative low density, ease of suspension, and high volume of large-sized organic material relative to inorganic (mineral) sediments of a similar size (i.e. material passing through the same sieve). Two exceptions occurred for the 060724 and 060728 events for unknown reasons (Table V).

The range of recorded C:N ratios for the 181 samples was 4–28; the median value was 11.2 ± 2.2 (calculated for all fractions combined; white line in Figure 4a). The mean weighted C:N value for each of the 12 storms ranged between 7.5 and 15.3 (Table VI). The median C:N ratios for the 12 events increased with increasing size fraction (Table VI): approximately 6–13 (for the fine fraction), 14–19 (medium), and 15–33 (coarse). These relationships are understandable when viewing scatterplots of the C:N values for all 181 samples, partitioned by size fraction, and plotted *versus* logged Q and TSS (Figure 4c,d). First, the C:N ranges for fine, median, and coarse fractions were quite different: 3–16, 12–25, and 8–83, respectively; associated medians were 9.3 ± 1.8, 16.7 ± 1.5, and 22.6 ± 4.5, respectively (Figure 4a). In addition, the very high values associated with large material were found for a wide range of TSS concentrations and flows (Figures 4c, d). A reasonable indicator for high C:N ratios for the coarse fraction was the percentage concentration of POC to TSS (the relationship is logged in Figure 4b)—however, the best fit exponential regression line only had an R^2 of 0.32 (significant at $\alpha = 0.05$). The coefficients of determination for the fine and medium fraction were very low ($R^2 \leq 0.1$; significant at $\alpha = 0.05$; not shown).

POC and PON relationships with flow, turbidity, and TSS

Particulate carbon and nitrogen did not exhibit a strong 'predictive' relationship with discharge (Figure 5a,d). Regression coefficients of determination were <0.25 for both POC and PON (not shown in Figure 5a,d). While POC and PON concentrations generally increased with Q, some of the highest concentrations were observed at low (<5 $m^3 s^{-1}$) to moderate (5–15 $m^3 s^{-1}$) flows (Figure 5a,d). A primary cause of the poor relationship between Q and

Table IV. Percentages of fine, medium, and coarse material comprising particulate organic carbon (POC), particulate organic nitrogen (PON), and total suspended solids (TSS) concentrations during the 12 monitored storms

Event	*n*	POC_{Fine}	POC_{Med}	POC_{Coarse}	POC_{All}	PON_{Fine}	PON_{Med}	PON_{Coarse}	PON_{All}	TSS_{Fine}	TSS_{Med}	TSS_{Coarse}	TSS_{All}
		%	%	%	mg C l^{-1}	%	%	%	mg N l^{-1}	%	%	%	mg l^{-1}
60724	11.0	90.4	4.8	1.8	42	98.0	2.8	0.5	5	76.2	14.1	0.5	736
60728	10.0	95.1	2.8	0.7	31	98.1	1.2	0.2	4	94.9	3.2	0.4	691
60808	12.0	53.6	26.6	9.1	44	69.7	17.1	3.9	4	35.8	52.0	1.3	1268
60908	20.0	55.6	39.7	3.9	31	67.5	31.0	2.1	2	48.6	37.7	0.5	1396
60909	11.0	71.8	21.7	2.4	24	83.1	13.3	1.3	2	65.0	23.7	0.5	1113
60912	14.0	56.3	35.7	5.2	72	63.9	28.5	2.2	5	44.4	42.8	0.5	3763
70504	12.0	54.0	35.7	5.4	26	57.7	24.4	3.1	2	71.2	23.2	1.1	699
70614	16.0	65.2	28.2	2.3	29	71.7	24.9	1.5	2	67.0	27.5	0.6	1055
70709	8.0	61.6	20.9	1.1	22	83.1	10.3	0.6	3	82.7	11.9	0.5	508
70822	16.0	76.0	8.8	1.0	45	80.2	4.4	0.5	6	93.2	3.8	0.3	1238
70823	18.0	70.7	15.5	1.1	48	78.5	7.2	0.6	6	91.3	10.7	0.3	1230
70828	12.0	60.2	29.0	2.8	66	78.0	19.8	1.3	7	75.5	36.9	0.4	2390

*POC_{All}, PON_{All}, and TSS_{All} are the medians of the '*n*' measured concentrations during the 12 storms (these data are not shown). Each of the percentages for fine, medium, and course fractions is a median of *n* event values; therefore, the percentages do not always sum to 100% (data are not shown). The Event ID is the date (year, month, day).

Table V. Percent contribution of fine, medium, and coarse fractions of particulate organic carbon (POC) and nitrogen (PON) to the total suspended solids (TSS) fractions

Event	n	POC_{Fine}/TSS_{Fine}	POC_{Med}/TSS_{Med}	$POC_{Coarse}/TSS_{Coarse}$	PON_{Fine}/TSS_{Fine}	PON_{Med}/TSS_{Med}	$PON_{Coarse}/TSS_{Coarse}$
		%	%	%	%	%	%
60724	11	7	2	19	0.83	0.13	0.57
60728	10	5	4	8	0.66	0.25	0.35
60808	12	5	2	24	0.66	0.11	1.01
60908	20	3	2	18	0.22	0.13	0.73
60909	11	2	2	10	0.25	0.11	0.46
60912	14	2	2	22	0.20	0.09	0.67
70504	12	3	6	19	0.27	0.35	0.96
70614	16	3	3	11	0.24	0.20	0.57
70709	8	3	7	9	0.50	0.43	0.63
70822	16	3	8	11	0.41	0.54	0.77
70823	18	3	6	13	0.39	0.30	0.85
70828	12	2	2	21	0.29	0.15	0.99

*Values are medians of n measurements during the 12 storms. The Event ID is the date (year, month, day).

Table VI. Carbon:nitrogen ratios for fine, medium, coarse, and all organic material

Event	n	$POC_{Fine}:PON_{Fine}$*	$POC_{Med}:PON_{Med}$*	$POC_{Coarse}:PON_{Coarse}$*	$C:N_{weighted}$+
		—	—	—	—
60724	11	8.1	14.9	33.1	10.3
60728	10	6.8	15.7	22.3	7.5
60808	12	7.8	15.8	23.8	12.1
60908	20	11.2	17.4	25.1	14.8
60909	11	9.7	18.3	21.5	12.6
60912	14	12.5	17.8	32.6	15.3
70504	12	10.4	16.2	19.4	12.0
70614	16	11.6	14.4	19.6	12.8
70709	8	6.4	17.6	15.0	8.0
70822	16	7.2	15.2	14.7	9.1
70823	18	7.9	18.9	15.9	11.9
70828	12	7.5	14.2	21.0	10.6

*Values are the medians of n measurements for each of the 12 storms.
+ $C:N_{weighted}$ was calculated as a weighted mean, based on discharge between the time of the first and last measurements during each storm. The Event ID is the date (year, month, day).

these variables is revealed in the storm event time series (Figure 3). Of the 12 events, 8 exhibited a delay in the POC and PON peaks relative to the Q peak (mean = 37 min)—producing peaks on the falling limb of the hydrograph, a response commonly observed for total particulate solids in general (Asselman, 1999; Jansson, 2002; Hudson, 2003; Coynel *et al*., 2005; Smith and Dragovich, 2009).

Turbidity had a greater correlation with POC and PON than discharge (Figure 5b,e). The strong linear increase with turbidity ($R^2 = 0.77$–0.81; linear regression on log-transformed data; $\alpha = 0.05$) is consistent with the strong correlation between TSS and turbidity observed in this catchment (Ziegler *et al*., 2014b) and elsewhere (Gippel, 1995; Stubblefield *et al*., 2007). Not surprising, therefore, POC and PON concentrations had a strong association with TSS ($R^2 = 0.85$ and 0.76, respectively; significant at $\alpha = 0.05$; Figures 5c,f).

The relationship between TSS and fine, medium, and coarse fractions of POC and PON is shown in Figure 6 (all values are log-transformed). The strongest relationships were between TSS and the medium fractions ($R^2 = 0.79$ for both POC and PON; significant at $\alpha = 0.05$; Figure 6b,e). The regression coefficients of determination for TSS *versus* fine size fractions of POC ($R^2 = 0.77$) and PON ($R^2 = 0.67$) were only slightly lower (significant at $\alpha = 0.05$; Figure 6a, d). However, both coarse fractions of POC and PON were not strongly correlated with TSS ($R^2 \leq 0.36$ for both; significant at $\alpha = 0.05$; Figure 6). Finally, all fractions of POC and PON were strongly correlated with each other

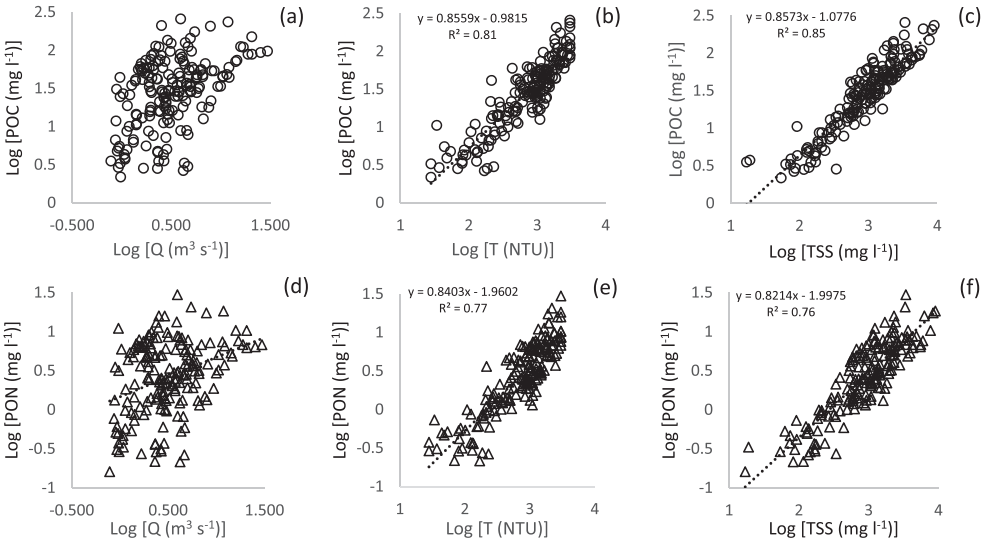

Figure 5. Relationships between discharge (Q), turbidity (T), and total suspended solids (TSS) and both particulate organic carbon (POC; panels a,b,c) and particulate organic nitrogen (PON; panels d,e,f). For POC and PON, all size fractions are combined

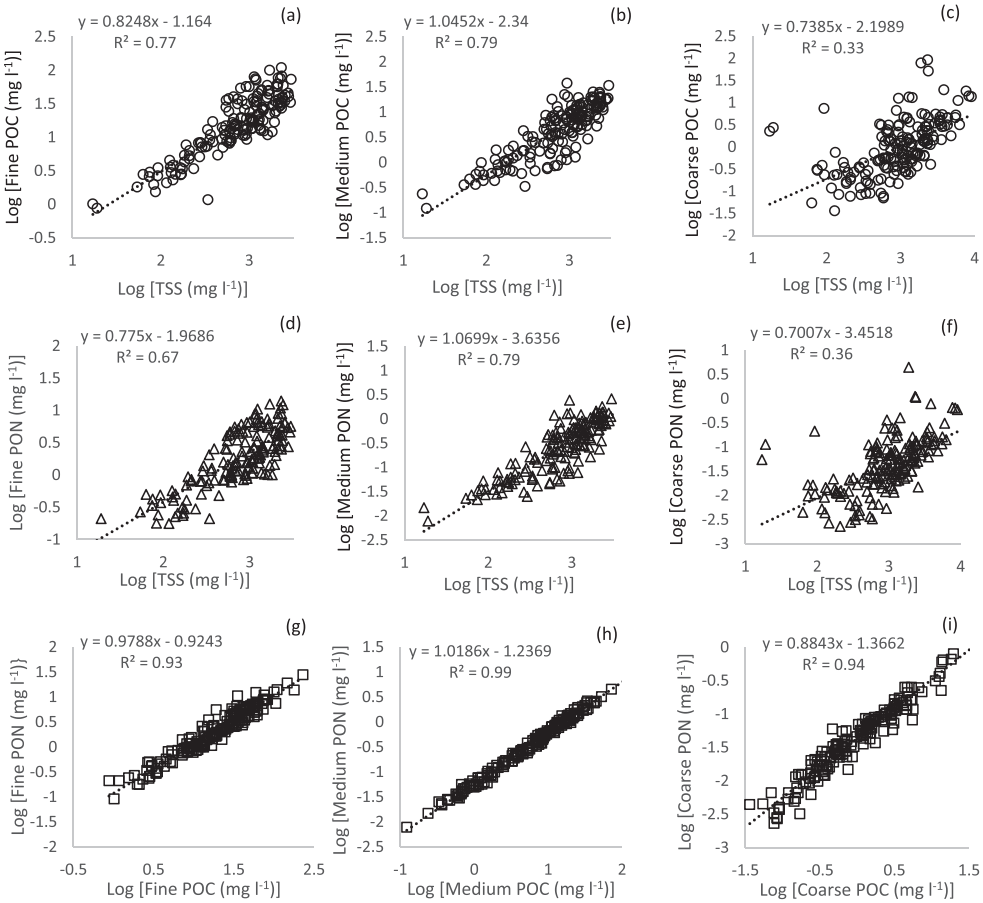

Figure 6. Relationship between total suspended solids (TSS) and particulate carbon concentration (POC, panels a–c) and particulate organic nitrogen (PON, panels d–f), partitioned by three size fractions. In panels g–i, the near-linear relationships between log-transformed POC and PON for three size fractions are shown. In all panels, size fractions are: coarse (>2000 μm), medium (63–2000 μm), and fine (0.7–63 μm)

(linear regression $R^2 > 0.94$ on log-transformed data; significant at $\alpha = 0.05$; Figure 6g–i).

Storm event hysteresis

Hysteresis refers to a non-uniform association between particulate matter and discharge, often on rising *versus* falling limbs (Walling, 1974). In general, anti-clockwise hysteresis can occur when the particulate source is far from the measurement location, the main material sources are valley slopes rather than the stream system, the supply of material in the stream does not become exhausted during the event, or a phenomenon such as stream bank collapse replenishes the supply of transported material without additional flow input occurring (Walling and Webb, 1987; Lenzi and Marchi, 2000; Lawler, *et al*., 2006; Rodriguez-Blanco *et al*., 2010). Clockwise hysteresis is often associated with a flushing of material within the channel or on the channel bank during the rising limb of the hydrograph (Walling, 1974, Asselman, 1999; Picouet *et al*., 2001; Hudson, 2003; Stubblefield *et al*., 2007).

We observed hysteresis between Q and the two variables POC and PON (Figure 7). In cases where the hydrograph was complex (e.g. exhibiting multiple peaks), hysteretic behaviour was also complex (for example event 070614; compare Figures 3h and 7h). In instances where the storm hydrograph exhibited a single discharge peak, the maximum concentration in POC often occurred on the falling limb of the hydrograph, producing an anti-clockwise hysteresis effect (060808, 060908, 060909, 070709, and 070822; Figures 7c,d,e,i,j). Storms exhibiting clockwise hysteresis were often those with the highest discharge (e.g. 060912 and 070823; Figures 7f,k). The complex hysteresis effect observed in two storms (e.g. 070614 and 070828; Figures 7h,l) was distinguished by changes between clockwise and anticlockwise hysteresis (Alexandrov *et al*. 2007; Duvert *et al*., 2010). In three other storms, a distinct type of hysteresis was not obvious (060724, 060728, and 070504; Figures 7b,g). Interestingly, all three of these events occurred early in the monsoon season, compared with other events monitored in their respective year. In general, hysteresis complicates the prediction of solid loads from discharge. More discussion on sediment hysteresis for this river is provided elsewhere (Ziegler *et al*., 2014b).

Annual POC and PON yields

Over the course of the study, the annual POC yield ranged from 5.0 to 22.3 Mg C km^{-2} y^{-1} (TSS-based estimate in Table II). In contrast, PON yield was a magnitude lower, ranging from 0.48 to 2.02 Mg N km^{-2} y^{-1} (Table II). The TSS- and T-based yields were comparable for years 2007 and 2008 (T-based estimate is the second listing in Table II). However, the 2006 yields were substantially different: 22.3 *versus* 15.9 Mg C km^{-2} y^{-1} for POC; and 2.02 *versus* 1.50 Mg N km^{-2} y^{-1} for PON (Table II). These differences were the result of the 2006 time series having high TSS concentrations with turbidity values of 3000 NTU, which is the maximum value that the turbidity probe can register (see Ziegler *et al*., 2014b). Thus, POC and PON values at these time stamps with high TSS concentration were under-predicted by the turbidity-based method. This under-prediction highlights the limitation of using turbidity probes in streams with very high sediment concentrations.

Across the three years investigated, 69–75% of the POC load was fine material, with medium (23–27%) and coarse (3–4%) fractions contributing smaller proportions (calculated from the values in Table II). PON demonstrated similar trends. The fine fraction comprised 80–84% of the loads in the three years while the medium (14–18%) and coarse fractions (1–2%) made up much smaller proportions (Table II). In comparison, the median fine, medium, and coarse contributions to the total measured POC concentrations were 71%, 23%, and 3%; and PON contributions were 81%, 15%, and 2% respectively in the 181 samples (not shown).

DISCUSSION

Comparison with other rivers

The Mae Sa 3-year POC yield estimates of 5.0–22.3 Mg C km^{-2} y^{-1} (Table II) are comparable with the yields in the Salween (8.8–12.5 Mg C km^{-2} y^{-1}) and Irrawaddy (5.3–10.4 Mg C km^{-2} y^{-1}) Rivers in Myanmar, the Capesterre River of Guadeloupe (8.1–25.5 Mg C km^{-2} y^{-1}), the Strickland (13 Mg C km^{-2} y^{-1}) River in Papua New Guinea, and the Mameyes (6.04 Mg C km^{-2} y^{-1}) Rivers in Puerto Rico (Table I). These rivers display similar TSS yields as Mae Sa (maximum < 850 Mg C km^{-2} y^{-1}; Table I). The Icacos (2.0–21.48 Mg C km^{-2} y^{-1}) and Cayaguas (19.16 Mg C km^{-2} y^{-1}) Rivers in Puerto Rico and Sepik River in Papua New Guinea (17.1 Mg C km^{-2} y^{-1}) have comparable POC yields (Table I), but TSS yields are much higher than in Mae Sa (>Mg C km^{-2} y^{-1}; Table I). The POC yield in the cleared Sungai Gombak catchment in Malaysia (6.16 Mg C km^{-2} y^{-1}) is comparable to that of Mae Sa in 2008, as was that of the Indravati and Pranhita Rivers of India (5.68–7.13 Mg C km^{-2} y^{-1}; Table I). The larger Loungchuanjiang (China) and the Ganges/Brahmaputra (India/Bangladesh) POC yield values are also similar (3.75–5.22 Mg C km^{-2} y^{-1}) to the lowest value for Mae Sa (Table I).

In contrast, the Mae Sa POC yield is much less than in the Lanyang-Hsi and Gaoping Rivers of Taiwan (23.0–69.2 Mg C km^{-2} y^{-1}), which have much higher TSS yields (Table I).

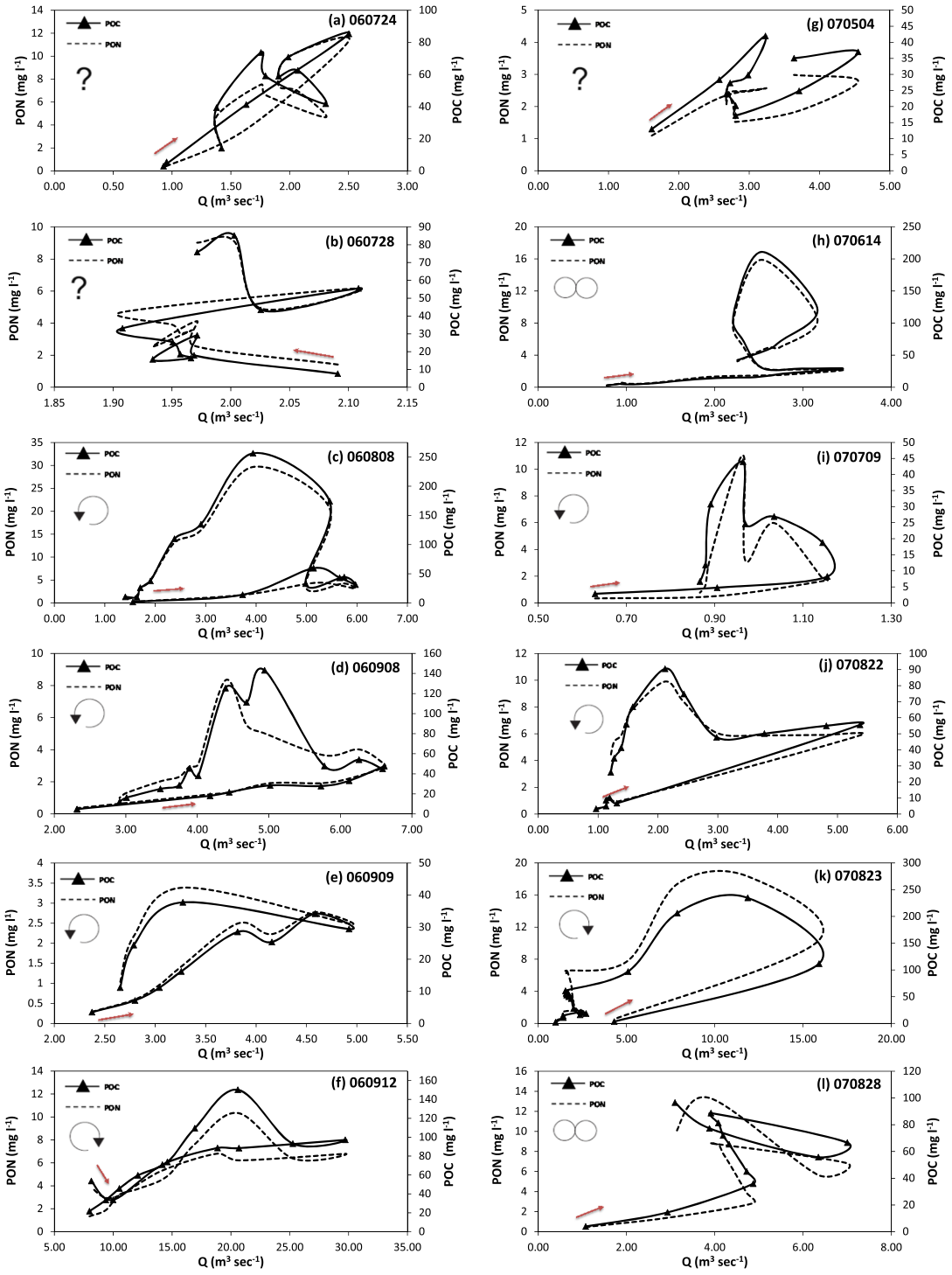

Figure 7. Hysteretic behaviour of particulate organic carbon (POC), particulate organic nitrogen (PON) and discharge (Q) during monitored storm events. Events 060808 (panel c), 060908 (d), 060909 (e), 070709 (i), 070822 (j) demonstrated anti-clockwise hysteresis; 060912 (f) and 070823 (k) demonstrated clockwise hysteresis; 070614 (h) and 070828 (l) complex hysteresis; and 060724 (a), 060728 (b), and 070504 (g) uncertain hysteresis. The small arrow indicates the start of the event and the initial change in the POC and PON values. Event IDs refer to year, month, and day

The Mae Sa POC yield is also less than the extremely high values reported for several New Zealand rivers and several rivers draining to the sea on the island of Timor (range = 43–238 Mg C km^{-2} y^{-1}; Table I). Most of these rivers have suspended solid loads that are two orders of magnitude higher than the Mae Sa. Thus, much higher POC loads are expected.

The Mae Sa PON range estimate of 0.48–2.02 Mg N km^{-2} y^{-1} is comparable with a few rivers systems worldwide

(Table I): the Capesterre River in Guadeloupe (0.55–1.70 Mg N km^{-2} y^{-1}); the Irrawaddy River in Myanmar (0.9 Mg N km^{-2} y^{-1}); the Ganges/Brahmaputra system (0.5–0.8 Mg N km^{-2} y^{-1}); and the Fly and Sepik Rivers in Papua New Guinea (1.6–1.7 Mg N km^{-2} y^{-1}). The Lanyang-Hsi River in Taiwan has a much higher PON yield (4.7 Mg N km^{-2} y^{-1})—but even this value is dwarfed by the estimated 49 Mg N km^{-2} y^{-1} for several rivers draining to the oceans surrounding Timor. The other rivers with PON estimations have much lower yields than Mae Sa (Table I: 0.032–0.3 Mg N km^{-2} y^{-1}). The model-simulated PON values for the Salween, Irrawaddy, Ganges/Brahmaputra, Yangtze, and Godavari (range = 0.2–0.9 Mg N km^{-2} y^{-1}) are reasonably similar to the lowest Mae Sa PON value (0.48 Mg N km^{-2} y^{-1}) in 2008, as is the 0.24 Mg N km^{-2} y^{-1} yield for the Longchuanjiang River of China.

Based on the limited amount of work done in the region, the POC contribution to TSS in Mae Sa (POC/TSS = 2.7–3.2% or 0.027–0.032; TSS-based estimate in Table II) is higher than that for most large river systems in Asia, with the exception being the Salween of Myanmar (0.054); a few rivers have values only slightly lower (Table I). Other rivers worldwide with much higher values include the following (Table I): the Capesterre (0.12); the Waikato (0.094); and the Fly (0.1). We originally believed our relatively high POC estimate was a function of high TSS loads. However, nearly all of the inland river systems in Asia with high TSS and particulate carbon yields have lower POC/TSS (e.g. those in China, India, Pakistan, Cambodia; Table I). In those systems, high erosion rates are often associated with gullying and mass wasting processes that may deliver substantial volumes of low-nutrient subsoil material to the stream system.

In the Mae Sa Catchment, however, erosion is often limited to the nutrient-rich top soil on agricultural sites (having relatively high organic material). Some additional material is supplied to the stream by road-associated erosion and episodic mass wasting events (especially in 2006; Ziegler *et al.*, 2014b). In addition, farm practices often involve discarding unwanted vegetative material directly into the stream system where it is readily mobilized during runoff events. The combination of all these factors likely helps produce the comparatively high POC and PON loads we observed (Table I). Here, we also recognize the vast differences in determination methods between the studies and the need to exercise caution in direct comparisons.

The high POC and PON loads estimated for the first year (2006) decreased in the two subsequent years (Table II). In prior work, we determined that higher rainfall partially distinguished the first year from the latter two (Ziegler *et al.*, 2014b); this rainfall effect can be seen in the larger stream flows in 2006 (Figure 2). However, a greater cause of the change over time was probably the diminishing supply of sediment in the stream system. In 2005, several landslides provided ample sediment to sustain high yields for a period of a few years before sediment exhaustion reduced the TSS loads (Ziegler *et al.*, 2014b). Here, we conclude that the decline in POC and PON yields over time also resulted from the depletion of organic material, rather than changes in the POC/TSS or PON/TSS relationship from one year to another. This claim is supported by there being no statistical differences in measured POC/TSS or PON/TSS for 2006 *versus* 2007 (Mann–Whitney U-test; $\alpha = 0.05$; for 181 observation data points).

Carbon–nitrogen relationships

The C:N ratio of each sample is fundamentally related to the type(s) of vegetation and other material comprising it (Aitkenhead and McDowell, 2000). The ratio may also be an indicator of the degree of decomposition and quality of organic matter in the sample (Ostrowska and Porebska, 2015)—but this effect is difficult to discern unless all material has the same initial C:N value, which is unlikely in catchments with heterogeneous vegetation. Over time as organic matter decays, carbon is lost via respiration as CO_2 and nitrogen is broken down during mineralization (Manzoni and Porporato, 2009). This may occur *in situ* or as the material is transported through a river system. Decomposition rate is dependent on many factors including climate, litter quality, and the nature and abundance of the decomposer organisms (Aerts, 1997). Further, carbon and nitrogen losses are not linear (Ostrowska and Porebska, 2015). Carbon mass is typically lost faster than nitrogen mass in initial stages of decay (Prescott, 2005; Osman, 2012). Owing to all of these factors, differences in C:N ratios found in riverine particulate matter samples may indicate heterogeneity in (1) the type of material transported, or (2) the degree of decomposition that has taken place.

While the C:N ratio reflects both source material and/or in-stream processes, the short catchment residence times (a few hours) and general high turbidity (median turbidity = 940 NTU for the 181 samples) of the stream water in Mae Sa lead us to believe that in-stream processes do not strongly influence the C:N ratio, especially during the rainy season when the vast majority of the flux occurs. Therefore, the observed high C:N ratios in many of the coarse-grained samples likely indicates the presence of 'fresh' organic material that has not undergone extensive degradation (C:N median = 23; max = 83; Figure 4). Meanwhile, the fine- and medium-grained fractions may contain organic material that is more degraded, as suggested by lower ratios (C:N = 12–25 and 3–16 for medium and fine material, respectively; Figure 4). The C:N ratios of these fractions more closely resemble that of soil organic material or degraded litter (Batjes 1996). The fine fraction may also contain other

types of organic material with low C:N ratios, such as phytoplankton. The C:N ratio of phytoplankton ranges from 4.6 to 7.5 because of the presence of significant amount of proteins rich in nitrogen (Bordovskiy 1965; Muller 1977). We cannot rule out this possibility as some of our samples were collected from a stream-side location where phytoplankton potentially could have accumulated. However, this component might be more important during the dry season when TSS and turbidity are low, and greater light availability might lead to higher phytoplankton productivity (Kohler *et al.*, 2012). More likely, another source of material with low C:N ratios in the fine fraction could originate from villages or farming areas where urea and ammonia inputs are likely high (e.g. from fertilizers, livestock areas, or sewage).

The relationship between discharge and C:N (weighted by fraction mass) is nonlinear and reasonably strong ($R^2 = 0.68$; significant at $\alpha = 0.05$; Figure 8a). Low flow events typically produced C:N ratios that were less than 11, whereas the ratios for larger events were typically higher. A wide range of flows produced C:N ratios of approximately 12 (Figure 8a). The other panels of Figure 8 (b–d) show the control that size fraction percentage has on C:N. Clear is the positive nonlinear correlation between C:N and the medium fraction percentage (Figure 8c), as well as the negative linear relation between C:N and percentage of fine material (Figure 8b). Finally shown in Figure 8d is the lack of association between C:N and the coarse fraction percentage, which did not change significantly (~0.3–1.3%) from event to event.

Consideration of C:N ratios plotted against Q for individual storms provides some insight into processes that may control changes in the ratios during storms (Figure 9). Furthermore, consideration of the spatial distribution of rainfall provides insight into differences among storms (Figure 10). During the largest storm (060912), 24.1 mm of rainfall produced 3 mm of discharge, 580 Mg of TSS, 14 Mg of POC, and nearly 1 Mg of PON (Table III). The event also had the highest C:N ratio of 15.3 (Table VI; Figure 10). The plot of C:N *versus* Q shows a clockwise hysteresis effect (Figure 9f) that was characterized by high C:N ratios (>16) early in the event, which decreased rapidly then stabilized for high discharges ($>20\,m^3\,s^{-1}$); the ratios on the falling limb were slightly lower (Figure 9f). The diagram of the spatial distribution of rainfall for all events show that intense rainfall occurred throughout the entire catchment during this event (Figure 10). The hysteresis pattern was possibly associated with the early flushing of new (undecomposed) organic matter into the stream near the sampling location early during the event. The C:N ratio was then 'diluted' with the mixing of many

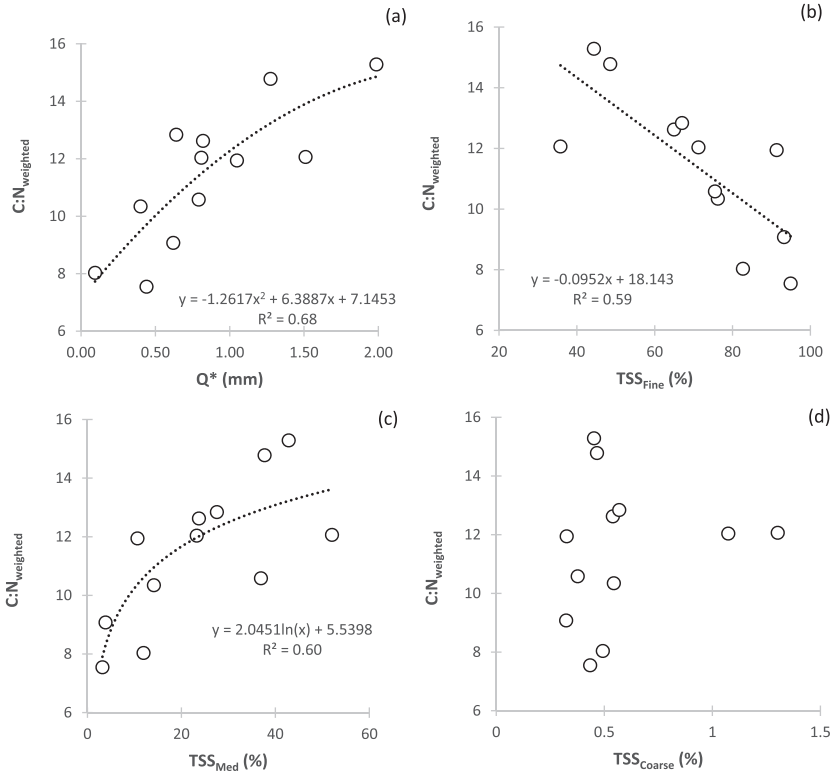

Figure 8. Relationship between event C:N(weighted by fraction) and (a) discharge (Q*); and total suspended solids of the (b) fine fraction (TSSfine); (c) medium fraction (TSSMed); and (d) coarse fraction (TSScoarse). Discharge (Q*) in this figure was determined only for the period between the first and last sampling occasions of TSS (thus, these discharge values are slightly different from those reported in Table III)

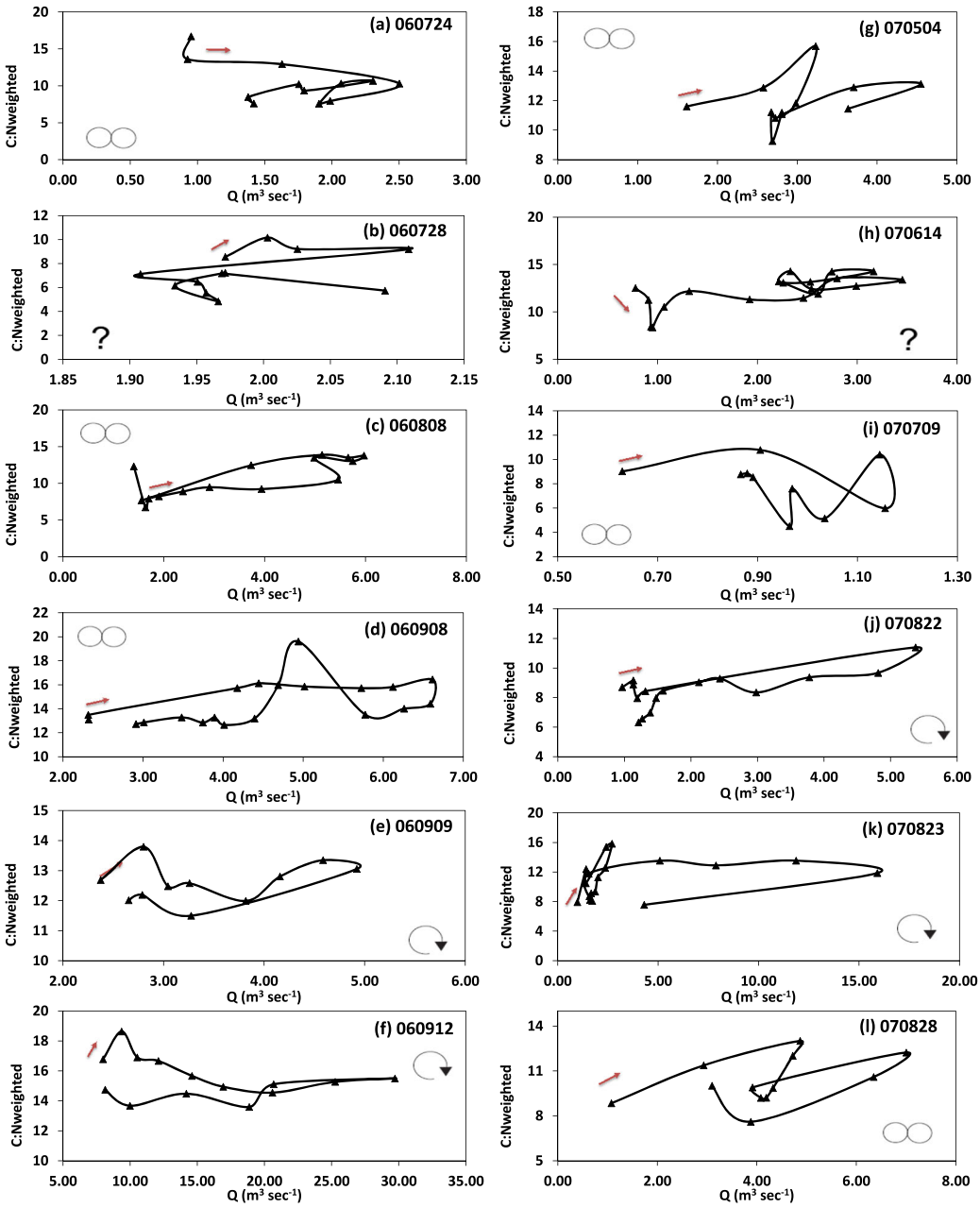

Figure 9. Hysteretic behaviour of C:N ratio of particulate organic matter and discharge (Q) during the 12 monitored storm events. Events 060909 (panel e), 060912 (f), 070822 (j), and 070823 (k) demonstrate clockwise hysteresis; 060724 (a), 060808 (c), 060908 (d), 070709 (i), 070504 (g), and 070828 (l) demonstrate complex hysteresis; 060728 (b) and 070614 (h) uncertain hysteresis. The small arrow indicates the start of the event and the initial change in the C:N values. Event IDs refer to year, month, and day

types of material of various states of decomposition from upstream locations. The contributions of fine and medium material to the total load during this event were nearly the same (44% and 43% respectively, Table IV). Thus, the transport of these fractions controlled the C:N signature throughout the event, although their weighting over time varied (not shown).

The C:N *versus* Q plots of all events reveal that both clockwise and complex hysteresis in the C:N ratio was common (Figure 9), and occurs for a wide range of storm sizes (Table III), in response to the variable spatial distribution in rainfall (Figure 10). Four of the 12 storms demonstrate clockwise hysteresis; six were complex (Figure 9). Some of these relationships could be classified as either because the patterns were associated with only a few data points (e.g. 060908 or 070709; Figures 9d,i) or with multiple peaks (e.g. 070504 and 070828; Figure 9 g,l). Of these, the event on 060908 is interesting in that it has

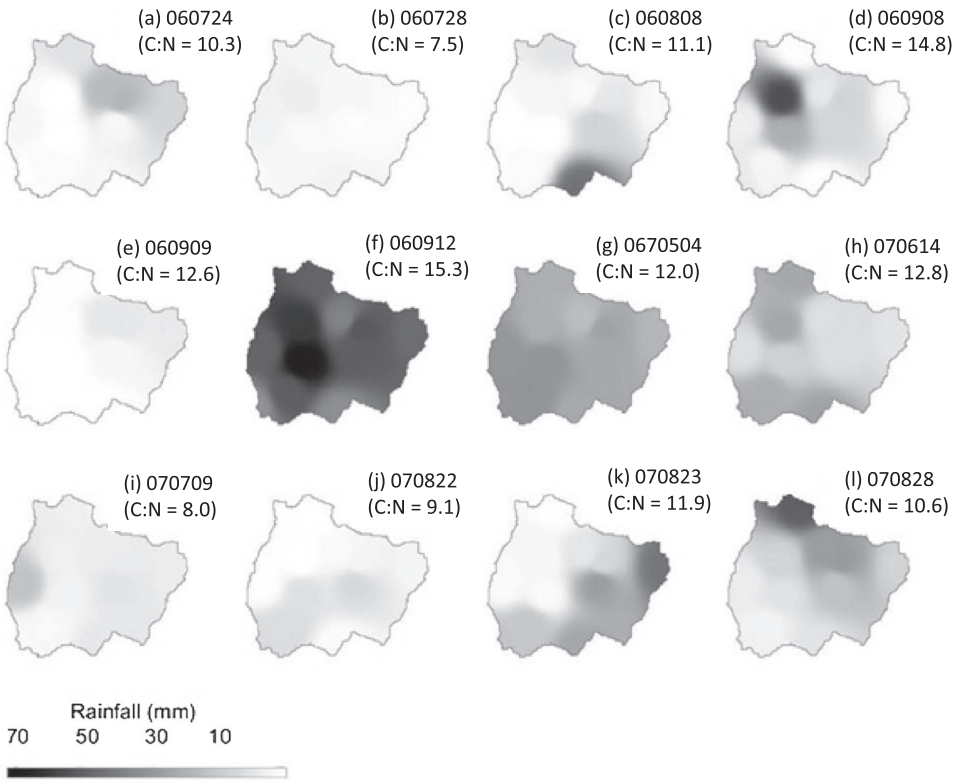

Figure 10. Spatial distribution of rainfall in Mae Sa Catchment for 12 storms in 2006 and 2007 (Table III). Also shown are the event C:N ratios (Table VI). Events with high C:N ratios are often associated with high intensity rainfall within some area of the catchment. Event IDs refer to year, month, and day

the second highest event C:N ratio (14.8) and is characterized by isolated intense rainfall in a forested part of the upper catchment (black patch in Figure 10d), that produced a high discharge with moderately high TSS, POC and PON loads (Table III). The distinct counter clockwise hysteresis in the POC and PON concentrations for this event (shown in Figure 7d) is related to the delay in the POC and PON peaks, relative to the discharge peak. The highest C:N value (~20; Figure 9d), which occurred on the falling limb, was elevated by a small amount of coarse material with a very high (C:N) ratio of 83 (not shown). The subsequent data point also has a high C:N ratio (~16, Figure 9d), again because of the presence of coarse, fresh material. This complex C:N pattern demonstrates the difficulty in predicting flushes of material of both different sizes and different geochemical signatures.

The rainfall magnitudes and distributions shown in Figure 10 provide support for the positive relationship between discharge and weighted C:N (shown in Figure 8 a). Most of the storms with high rainfall correspond with high C:N ratios (Figure 10). These large events typically produced higher discharges at the basin outlet. Nearly all of the events without intense rainfall had C:N ratios < 11, with event 060909 (Figure 10e) being an exception. Large events have the potential to initiate erosion, produce surface runoff capable of transporting sediment and organic material to the stream, dislodge vegetative material stored on stream banks, and blow fresh vegetative material into the stream directly. Consequently, it is logical that C:N has a positive association with rainfall intensities (inferred from Figure 8a and 10, but not calculated), as shown also in other studies (Valett *et al.*, 2008; Frost *et al.*, 2009; Gao *et al.*, 2014).

Collectively, the observed patterns support the existence of several phenomena: (1) events early in the rainy season may transport a higher percentage of material that has undergone substantial breakdown over the long dry period (e.g. the discarded agricultural litter mentioned above), whereas late-season storms may mobilize more 'new' material than has emerged during the wet season; (2) the early events may contain more plankton when turbidity is low and light availability high; (3) big storms (e.g. 060908, 060912, and 070823) can mobilize large, potentially less-decayed material that originates from high stream-side locations or is blown into the stream by strong winds (this assertion is supported by observations but not wind data); and (4) rainfall occurring in different areas of the catchment may mobilize material with different C:N ratios (e.g. forested *vs* agricultural areas).

With respect to the latter, the C:N ratio of the spatially isolated 060908 event in the forested upper catchment (see Figure 10d) was substantially higher than that for the 070828 event (Figure 10l), which had a wider spatial extent in the lower part of the catchment. The complex C:N hysteresis for the 070828 event was characterized by multiple flushes of material with relatively high C:N ratios (Figure 9l). The high values are likely associated with fresh material transported from various locations of the catchment with different land uses and/or land covers. Additional work using stable isotopes of carbon and nitrogen would be useful for exploring this issue further.

CONCLUSIONS

This study provides some of the first particulate carbon and nitrogen yield estimates for a headwater catchment on the Asian continent. The calculated yield estimates indicate that the Sa River is an important source of POC and PON flowing into larger rivers that drain to downstream rivers, reservoirs, and the ocean. The POC contribution to the total suspended solid load (roughly 3% across three years) is high compared with larger rivers on the Asian continent that flow to the ocean. Thus, while headwater streams such as Mae Sa may be hotspots for particulate matter entering larger systems, some of this material may be sequestered in downstream reservoirs before reaching the coast.

The substantial contribution of material >63 μm (~25–31%) to the POC and PON loads is likely the product of the transport of fresh vegetative material to the stream, particularly during the wettest parts of the rainy season. The highest C:N ratios are for the coarsest fractions of material sampled, indicating the transport of new vegetative material, as opposed to older, more decomposed material. Nevertheless, the great contribution of fine material to the overall TSS loads during storms largely determines both the total loads and the C:N signatures during storms.

With respect to inter- and intra-storm variation, particulate carbon and nitrogen flux exhibits a complex relationship with storm discharge, as peak concentrations in particulate carbon and nitrogen are often delayed relative to flow peaks. This complex behaviour, often marked by hysteresis, limits the usefulness of discharge as a predictive variable of POC and PON fluxes. Hysteresis also occurs with respect to C:N ratios. Turbidity, a parameter easily measured automatically and continuously, is useful for estimating annual or multi-year particulate carbon and nitrogen yields—but not when turbidity measurements exceed the limit of the recording instrument, which is often a common problem in small streams with significant erosion occurring.

ACKNOWLEDGEMENTS

This work was funded by grants from the National University of Singapore (R-109-000-090-112, R-109-000-134-112, R-109-000-109-646), Asia Pacific Network (ARCP2008-01CMY) and NASA (#NNX08AL90G). We also recognize the contributions of Tom Giambellcua, Mike Nullet, and Jefferson Fox.

REFERENCES

Aerts R. 1997. Climate, leaf litter chemistry and leaf litter decomposition in terrestrial ecosystems: a triangular relationship. *Oikos* **79**: 439–449. DOI:10.2307/3546886

Aitkenhead JA, McDowell WH. 2000. Soil C:N ratio as a predictor of annual riverine DOC flux at local and global scales. *Global Biogeochemical Cycles* **14**: 127–138.

Aldrian E, Chen C-TA, Adi S, Prihartanto SN, Nugroho SP. 2008. Spatial and seasonal dynamics of riverine carbon fluxes of the Brantas catchment in East Java. *Journal of Geophysical Research* **113**: G03029. DOI:10.1029/2007JG000626

Alexandrov Y, Laronne JB, Reid I. 2007. Intra-event and inter-seasonal behavior of suspended sediment in flash floods of the semi-arid northern Negev, Israel. *Geomorphology* **85**: 85–97.

Alford D. 1992. Streamflow and sediment transport from mountain watersheds of the Chao Phraya Basin, Northern Thailand: a reconnaissance study. *Mountain Research and Development* **12**: 257–268.

Ahnert F. 1970. Functional relationships between denudation, relief, and uplift in large mid-latitude drainage basins. *American Journal of Science* **268**: 243–263. DOI:10.2475/ajs.268.3.243

Alin SR, Aalto R, Goni MA, Richey JE, Dietrich WE. 2008. Biogeochemical characterization of carbon sources in the Strickland and Fly Rivers, Papua New Guinea. *Journal of Geophysical Research* **113**: F01S05. DOI:10.1029/2006JF000625

Alongi DM, da Silva M, Wasson RJ, Wirasantosa S. 2013. Sediment discharge and export of fluvial carbon and nutrients into the Arafura and Timor Seas: a regional synthesis. *Marine Geology* **343**: 146–158. DOI:10.1016/j.margeo.2013.07.004

Asselman NEM. 1999. Suspended sediment dynamics in a large drainage basin: the River Rhine. *Hydrological Processes* **13**: 1437–1450. DOI:10.1002/(SICI)1099-1085(199907)13:10<1437::AID-HYP821>3.0.CO;2-J

Atapattu SS, Kodituwakku DC. 2009. Agriculture in South Asia and its implications on downstream health and sustainability: a review. *Agricultural Water Management* **96**: 361–373. DOI:10.1016/j.agwat.2008.09.028

Aucour AM, France-Lanord C, Pedoja K, Pierson-Wickman A-C, Sheppard SMF. 2006. Fluxes and sources of particulate organic carbon in the Ganga-Brahmaputra. *Global Biogeochemical Cycles* **20**: BG2006. DOI:10.1029/2004GB002324

Balakrishna K, Probst JL. 2005. Organic carbon transport and C:N ratio variations in a large tropical river: Godavari as a case study, India. *Biogeochemistry* **7**: 457–473. DOI:10.1007/s10533-004-0879-2

Bannwarth MA, Sangchan W, Hugenschmidt C, Lamers M, Ingwersen J, Ziegler AD, Streck T. 2014a. Pesticide transport simulation in a tropical catchment by SWAT. *Environmental Pollution* **191**: 70–79.

Bannwarth MA, Hugenschmidt C, Sangchan W, Lamers M, Ingwersen J, Ziegler AD, Streck T. 2014b. Simulation of stream flow components in a mountainous catchment in northern Thailand with SWAT, using the ANSELM calibration approach. *Hydrological Processes* **29**: 1340–1352. DOI:10.1002/hyp.10268

Bass AM, Bird MI, Liddell MJ, Nelson PN. 2011. Fluvial dynamics of dissolved and particulate organic carbon during periodic discharge in a steep tropical rainforest catchment. *Limnology and Oceanography* **56**: 2282–2292. DOI:10.4319/lo.2011.56.6.2282

Batjes NH. 1996. Total carbon and nitrogen in the soils of the world. *European Journal of Soil Science* **2**: 151–163. DOI:10.1111/j.1365-2389.1996.tb01386.x

Beusen AHW, Dekkers ALM, Bouwaman AF, Ludwig W, Harrison J. 2005. Estimation of global river transport of sediments and associated particulate C, N, and P. *Global Biogeochemical Cycles* **19**: DOI:10.1029/2005GB002453

Bird MI, Robinson RAJ, Oo N, Win A. 2008. Preliminary estimate of organic carbon transport by the Ayeyarwady (Irrawaddy) and Thanlwin (Salween) Rivers of Myanmar. *Quaternary International* **186**: 113–122. DOI:10.1016/j.quaint.2007.08.003

Bishop JE. 1973. *Limnology of a small Malayan river Sungai Gombak*. Junk Publishers, The Hague: Dr. W.

Bordovskiy OK. 1965. Sources of organic matter in marine basins. *Marine Geology* **3**: 5–31.

Bruun TB, De Neergaard A, Lawrence D, Ziegler AD. 2009. Environmental consequences of the demise in Swidden Agriculture in SE Asia: soil nutrients and carbon stocks. *Human Ecology* **37**: 375–388. DOI:10.1007/s10745-009-9257-y

Burns KA, Brunskill G, Brinkman D, Zagorskis I. 2008. Organic carbon and nutrient fluxes to the coastal zone from the Sepik River outflow. *Continental Shelf Research* **28**: 283–301. DOI:10.1016/j.csr.2007.08.004

Capone DG, Bronk DA, Muholland MR, Carpenter EJ. 2008. *Nitrogen in the marine environment*. Academic Press: Academic Press, Elsevier, Amesterdam; 1757.

Coynel A, Seyler P, Etcheber H, Meybeck M, Orange D. 2005. Spatial and seasonal dynamics of total suspended sediment and organic carbon species in the Congo River. *Global Biogeochemical Cycles* 19. DOI:10.1029/2004GB002335

Dadson SJ, Hovius N, Chen H, Dade WB, Hsieh M-L, Willet SD, Hu J-C, Horng MJ, Chen M-C, Start CP, Lague D, Lin J-C. 2003. Links between erosion, runoff variability and seismicity in the Taiwan orogen. *Nature* **426**: 648–651. DOI:10.1038/nature02150

Duvert C, Gratiot N, Evrard O, Navratil O, Nemery J, Prat C, Esteves M. 2010. Drivers of erosion and suspended sediment transport in three headwater catchments of the Mexican Central Highlands. *Geomorphology* **123**: 243–256. DOI:10.1016/j.geomorph.2010.07.016

Douglas I. 1996. The impact of land-use changes, especially logging, shifting cultivation, mining and urbanization on sediment yields in human tropical Southeast Asia: a review with special reference to Borneo. Erosion and sediment yield: global and regional perspectives (proceedings of the Exeter symposium, July 1996). *IAHS Publication* **236**: 463–471.

Ellis EE, Keil RG, Ingalls AE, Richey JE, Alin SR. 2012. Seasonal variability in the sources of particulate organic matter of the Mekong River as discerned by elemental and lignin analyses. *Journal of Geophysical Research, Biogeosciences* **117**: G01038. DOI:10.1029/2011JG001816

FAO 2014. IUSS Working Group WRB. World Reference Base for Soil Resources 2014. International soil classification system for naming soils and creating legends for soil maps. World Soil Resources Reports No. 106. FAO, Rome.

Finlayson DP, Montgomery DR, Hallet B. 2002. Spatial coincidence of rapid inferred erosion with young metamorphic massifs in the Himalayas. *Geology* **30**: 219–222. DOI:10.1130/0091-7613(2002)030<0219:SCORIE>2.0.CO;2

Frost PC, Kinsman LE, Johnston CA, Larson JH. 2009. Watershed discharge modulates relationships between landscape components and nutrient ratios in stream seston. *Ecology* **90**: 1631–1640.

Gao Y, Zhub B, Yua G, Chenc W, Hea N, Wangb T, Miaod C. 2014. Coupled effects of biogeochemical and hydrological processes on C, N, and P export during extreme rainfall events in a purple soil watershed in southwestern China. *Journal of Hydrology* **511**: 692–702. DOI:10.1016/j.jhydrol.2014.02.005

Gao QZ, Tao Z, Shen C, Sun Y, Yi W, Xing C. 2002. Riverine organic carbon in the Xijiang River (South China): seasonal variation in content and flux budget. *Environmental Geology* **41**: 826–832. DOI:10.1007/s00254-001-0460-4

Gao QZ, Tao Z, Yao GR, Ding J, Liu ZF, Liu KX. 2007. Elemental and isotopic signatures of particulate organic carbon in the Zengjiang River, southern China. *Hydrological Processes* **21**: 1318–1327. DOI:10.1002/hyp.6358

Gippel CJ. 1995. Potential of turbidity monitoring for measuring the transport of suspended-solids in streams. *Hydrological Processes* **9**: 83–97. DOI:10.1002/hyp.3360090108

Gomez B, Trustrum NA, Hicks DM, Rogers KM, Page MJ, Tate KR. 2003. Production, storage, and output of particulate organic carbon: Waipaoa River basin, New Zealand. *Water Resources Research* **39**: 1161. DOI:10.1029/2002WR001619

Gruber N, Galloway JN. 2008. An earth-system perspective of the global nitrogen cycle. *Nature* **451**: 293–296. DOI:10.1038/nature06592

Gupta A. 1996. Erosion and sediment yield in Southeast Asia: a regional perspective. Erosion and Sediment Yield: Global and Regional Perspectives. Proceedings of the Exeter Symposium, July 1996. *IAHS Publication* **236**: 215–222.

Hicks DM, Gomez B, Trustrum NA. 2000. Erosion thresholds and suspended sediment yields, Waipaoa river basin. *New Zealand. Water Resources Research* **36**: 1129–1142.

Hicks DM, Gomez B, Trustrum NA. 2004. Event suspended sediment characteristics and the generation of hyperpycnal plumes at river mouths: East Coast Continental Margin, North Island. *New Zealand Journal of Geology* **112**: 471–485. DOI:10.1086/421075

Hilton RG, Galy A, Hovius N. 2008. Riverine particulate organic carbon from an active mountain belt: importance of landslides. *Global Biogeochemical Cycles* **22**: GB1017. DOI:10.1029/2006GB002905

Hilton RG, Galy A, Hovius N, Horng MJ, Chen H. 2010. The isotopic composition of particulate organic carbon in mountain rivers of Taiwan. *Geochimica et Cosmochimica Acta* **74**: 3164–3181. DOI:10.1016/j.gca.2010.03.004

Hudson PF. 2003. Event sequence and sediment exhaustion in the lower Panuco Basin, Mexico. *Catena* **52**: 57–76. DOI:10.1016/S0341-8162(02)00145-5

Huang T-H, Fu Y-H, Pan P-Y, Chen CTA. 2012. Fluvial carbon fluxes in tropical rivers. *Current Opinions in Environmental Sustainability* **4**: 162–169. DOI:10.1016/j.cosust.2012.02.004

Hung J-J, Yeh Y-T, Huh C-A. 2012. Efficient transport of terrestrial particulate carbon in a tectonically-active marginal sea off southwestern Taiwan. *Marine Geology* **315-318**: 29–43. DOI:10.1016/j.margeo.2012.05.006

Ittekkot V, Zhang S. 1989. Pattern of particulate nitrogen transport in world rivers. *Global Biogeochemical Cycles* **3**: 383–391.

Jansson MB. 2002. Determining sediment source areas in a tropical river basin, Costa Rica. *Catena* **47**: 63–84. DOI:10.1016/S0341-8162(01)00173-4

Jennerjahn TC, Soman K, Ittekkot V, Nordhaus I, Sooraj S, Priya RS, Lahajnar N. 2008. Effect of land use on the biogeochemistry of dissolved nutrients and suspended and sedimentary organic matter in the tropical Kallada River and Ashtamudi estuary, Kerala. *India Biogeochemisty* **90**: 29–47. DOI:10.1007/s10533-008-9228-1

Jickells TD. 1998. Nutrient biogeochemistry of the coastal zone. *Science* **281**: 217–222. DOI:10.1126/science.281.5374.217

Kao SJ, Liu KK. 1996. Particulate organic carbon export from a subtropical mountainous river (Lanyang Hsi) in Taiwan. *Limnology and Oceanography* **41**: 1749–1757. DOI:10.4319/lo.1996.41.8.1749

Kao SJ, Liu KK. 2000. Stable carbon and nitrogen isotope systematics in a human-disturbed watershed (Lanyang-His) in Taiwan and the estimation of biogenic particulate organic carbon and nitrogen fluxes. *Global Biogeochemical Cycles* **14**: 189–198. DOI:10.1029/1999GB900079

Kineke GC, Wooslfe KJ, Kuehl SA, Milliman JD, Dellapenna TM, Purdon RG. 2000. Sediment export from the Sepik River, Papua New Guinea: evidence for a divergent sediment plume. *Continental Shelf Research* **20**: 2239–2266. DOI:10.1016/S0278-4343(00)00069-8

Kohler TJ, Heatherly TN, El-Sabaawi RW, Zandonà E, Marshall MC, Flecker AS, Pringle CM, Reznick DN, Thomas SA. 2012. Flow, nutrients, and light availability influence Neotropical epilithon biomass and stoichiometry. *Freshwater Science* **31**: 1019–34. DOI:10.1093/icb/ict057

Korup O, McSaveney MJ, Davies TRH. 2004. Sediment generation and delivery from large historic landslides in the Southern Alps, New Zealand. *Geomorphology* **61**: 189–207. DOI:10.1016/j.geomorph.2004.01.001

Lal R. 2003. Soil erosion and the global carbon budget. *Environment International* **29**: 437–450. DOI:10.1016/S0160-4120(02)00192-7

Lawler DM, Petts GE, Foster IDL, Harper S. 2006. Turbidity dynamics during spring storm events in an urban headwater river system: The Upper Tame, West Midlands, UK. *Science of the Total Environment* **360**: 109–126. DOI:10.1016/j.scitotenv.2005.08.032

Lenzi MA, Marchi L. 2000. Suspended sediment load during floods in a small stream of the Dolomites (northeastern Italy). *Catena* **39**: 267–282. DOI:10.1016/S0341-8162(00)00079-5

Liu C, Sui J, Wang ZY. 2008a. Changes in runoff and sediment yield along the Yellow River during the period from 1950 to 2006. *Journal of Environmental Informatics* **12**: 129–139.

Liu JP, Liu CS, Xu KH, Milliman JD, Chiu JK, Kao SJ, Lin SW. 2008b. Flux and fate of small mountainous rivers derived sediments into the Taiwan Strait. *Marine Geology* **256**: 65–76. DOI:10.1016/j.margeo.2008.09.007

Liu JT, Hung J-J, Lin H-L, Huh C-A, Lee C-L, Hsu RT, Huang Y-W, Chu JC. 2009. From suspended particles to strata: the fate of terrestrial substances in the Gaoping (Kaoping) submarine canyon. *Journal of Marine Systems* **76**: 417–432.

Lloret E, Dessert C, Lajeunesses E, Crispi O, Pastor L, Gaillardet J, Benedetti MF. 2012. Are small mountainous tropical watersheds of oceanic islands important for carbon export? *Biogeosciences Discussions* **9**: 7117–7163. DOI:10.5194/bgd-9-7117-2012

Ludwig W, Probst JL, Kempe S. 1996. Predicting the oceanic input of organic carbon by continental erosion. *Global Biogeochemical Cycles* **10**: 23–41. DOI:10.1029/95GB02925

Ludwig W, Amiotte-Suchet P, Munhoven G, Probst JL. 1998. Atmospheric CO2 consumption by continental erosion: present-day controls and implications for the last glacial maximum. *Global and Planetary Change* **17**: 107–120. DOI:10.1016/S0921-8181(98)00016-2

Lu XX, Li S, He M, Zhou Y, Bei RT, Ziegler AD. 2011. Seasonal changes of nutrients in the Upper Changjiang basin: an example of the Longchuanjiang River, China. *Journal of Hydrology* **405**: 344–351. DOI:10.1016/j.jhydrol.2011.05.032

Lu XX, Li S, He M, Zhou Y, Ziegler AD. 2012. Organic carbon fluxes from the upper Yangtze basin: example of the Longchuanjiang River, China. *Hydrological Processes* **26**: 1604–1616. DOI:10.1002/hyp.8267

Lyons WB, Nezat CA, Carey AE, Hicks DM. 2002. Organic carbon fluxes to the ocean from high-standing islands. *Geology* **30**: 443–446. DOI:10.1130/0091-7613(2002)030<0443:OCFTTO>2.0.CO;2

Lyons WB, Carey AE, Hicks DM, Nezat CA. 2005. Chemical weathering in high-sediment yielding watersheds, New Zealand. *Journal of Geophysical Research* **110**: F01008. DOI:10.1029/2003JF000088

Manzoni S, Porporato A. 2009. Soil carbon and nitrogen mineralization: theory and models across scales. *Soil Biology and Biochemistry* **41**: 1355–1379. DOI:10.1016/j.soilbio.2009.02.031

McDowell WH, Asbury CE. 1994. Export of carbon, nitrogen, and major ions from three tropical montane watersheds. *Limnology and Oceanography* **39**: 111–125. DOI:10.4319/lo.1994.39.1.0111

Mackenzie FT, Lerman A, Ver LMB. 1998. Role of the continental margin in the global carbon balance during the past three centuries. *Geology* **26**: 423–426. DOI:10.1130/0091-7613(1998)026<0423:ROTCMI>2.3.CO;2

Meybeck M. 1993. Riverine transport of atmospheric carbon—sources, global typology and budget. *Water, Air, and Soil Pollution* **70**: 443–463. DOI:10.1007/BF01105015

Meybeck M, Laroche L, Durr HH, Syvitski JPM. 2003. Global variability of daily total suspended solids and their fluxes in rivers. *Global Planetary Change* **39**: 65–93. DOI:10.1016/S0921-8181(03)00018-3

Milliman JD, Meade RH. 1983. World-wide delivery of river sediment to the oceans. *Journal of Geology* **91**: 1–21.

Moore S, Gauci V, Evans CD, Page SE. 2011. Fluvial organic carbon losses from a Bornean blackwater river. *Biogeosciences* **8**: 901–909. DOI:10.5194/bg-8-901-2011

Muller PJ. 1977. C:N ratios in Pacific deep-sea sediments: effect of inorganic ammonium and organic nitrogen compounds sorbed by clays. *Geochimica et Cosmochimica Acta* **41**: 765–776.

Murphy SF, Stallard RF. 2012. Water quality and landscape processes of four watersheds in eastern Puerto Rico. *US Geological Survey Professional* **1789**: 292.

Ni H-G, Lu F-H, Luo X-L, Tian H-Y, Zeng EY. 2008. Riverine inputs of total organic carbon and suspended particulate matter from the Pearl River Delta to the coastal ocean of South China. *Marine Pollution Bulletin* **56**: 1150–1157. DOI:10.1016/j.marpolbul.2008.02.030

Osman KT. 2012. Forest and forest soils are important carbon sequesters. In *Soils: principles, properties and management*. Springer Science & Business Media: London, UK; 263.

Ostrowska A, Porebska G. 2015. Assessment of the C/N ratio as an indicator of the decomposability of organic matter in forest soils. *Ecological Indicators* **49**: 104–109. DOI:10.1016/j.ecolind.2014.09.044

Panda DK, Kumar A, Mohanty S. 2011. Recent trends in sediment load of the tropical (Peninsular) river basins of India. *Global and Planetary Change* **75**: 108–118. DOI:10.1016/j.gloplacha.2010.10.012

Picouet C, Hingray B, Olivry JC. 2001. Empirical and conceptual modeling of the suspended sediment dynamics in a large tropical African river: the Upper Niger river basin. *Journal of Hydrology* **250**: 19–39. DOI:10.1016/S0022-1694(01)00407-3

Pimentel D, Harvey C, Resosudarmo P, Sinclaire K, Kurz D, McNair M, Crist S, Shpritz L, Fitton L, Saffouri R, Blair R. 1995. Environmental and economic costs of soil erosion and conservation benefits. *Science* **267**: 1117–1123. DOI:10.1126/science.267.5201.1117

Prescott CE. 2005. Do rates of litter decomposition tell us anything we really need to know? *Forest Ecology and Management* **220**: 66–74. DOI:10.1016/j.foreco.2005.08.005

Ran LS, Lu XX, Sun H, Han J, Li R, Zhang J. 2013. Spatial and seasonal variability of organic carbon transport in the Yellow River, China. *Journal of Hydrology* **498**: 76–88. DOI:10.1016/j.jhydrol.2013.06.018

Richey JE, Melack JM, Aufdenkampe AK, Ballester VM, Hess LL. 2002. Outgassing from Amazonian rivers and wetlands as a large tropical source of atmospheric CO_2. *Nature* **416**: 617–620. DOI:10.1038/416617a

Robinson RAJ, Bird MI, Win ON, Hoey TB, Aye MM, Higgitt DL, Lu XX, Swe A, Tun T, Win SL. 2007. The Irrawaddy River sediment flux to the Indian Ocean: the original nineteenth-century data revisited. *Journal of Geology* **115**: 629–640. DOI:10.1086/521607

Rodriguez-Blanco ML, Taboada-Castro MM, Taboada-Castro MT. 2010. Sources and sediment yield from a rural catchment in humid temperate environment, northwest Spain. *Earth Surface Processes and Landforms* **35**: 272–277. DOI:10.1002/esp.1906

Sarin MM, Sudheer AK, Balakrishna K. 2002. Significance of riverine carbon transport: a case study of a large tropical river, Godavari (India). *Science in China (Series C)* **45**: 97–108.

Schlunz B, Schneider RR. 2000. Transport of terrestrial organic carbon to the oceans by rivers: re-estimating flux- and burial rates. *International Journal of Earth Sciences* **88**: 599–606. DOI:10.1007/s005310050290

Schlesinger WH, Melack JM. 1981. Transport of organic carbon in the world's rivers. *Tellus* **33**: 172–187.

Seitzinger SP, Harrison JA, Dumont E, Beusen AHW, Bouwman AF. 2005. Sources and delivery of carbon, nitrogen, and phosphorus to the coastal zone: an overview of Global Nutrient Export from Watersheds (NEWS) models and their application. *Global Biogeochemical Cycles* **19**: DOI:10.1029/2005GB002606

Sidle RC, Ziegler AD. 2010. Elephant trail runoff and sediment dynamics in northern Thailand. *Journal of Environmental Quality* **39**: 871–881. DOI:10.2134/jeq2009.0218

Sidle RC, Ziegler AD. 2012. The dilemma of mountain roads. *Nature Geoscience* **5**: 437–438.

Smil V. 1999. Nitrogen in crop production: an account of global flows. *Global Biogeochemical Cycles* **13**: 647–662. DOI:10.1029/1999GB900015

Smith HG, Dragovich D. 2009. Interpreting sediment delivery processes using suspended sediment-discharge hysteresis patterns from nested upland catchments, south-eastern Australia. *Hydrological Processes* **23**: 2415–2426. DOI:10.1002/hyp.7357

Soil Survey Staff. 2014. Kellogg Soil Survey Laboratory Methods Manual. Soil Survey Investigations Report No. 42, Version 5.0. R. Burt and Soil Survey Staff (ed.). U.S. Department of Agriculture, Natural Resources Conservation Service.

Stubblefield AP, Reuter JE, Dahlgren RA, Goldman CR. 2007. Use of turbidometry to characterize suspended sediment and phosphorus fluxes in the Lake Tahoe basin, California, USA. *Hydrological Processes* **21**: 281–291. DOI:10.1002/hyp.6234

Summerfield MA, Hulton NJ. 1994. Natural controls of fluvial denudation rates in major world drainage basins. *Journal of Geophysical Research-Solid Earth* **99**: 13871–13883. DOI:10.1029/94JB00715

Sun HG, Han JT, Zhang SR, Lu XX. 2007. The impacts of "05.6" extreme flood event on riverine carbon fluxes in Xijiang River. *Chinese Science Bulletin* **52**: 805–812.

Thompson CE. 2009. Tracking Organic Matter from Source to Sink in the Waiapu River Watershed. *New Zealand: A Geochemical Perspective*. PhD Dissertation. North Carolina State University: Raleigh NC, USA; 335 p.

Valett HM, Thomas SA, Mulholland PJ, Webster JR, Dahm CN, Fellows CS, Crenshaw CL, Peterson CG. 2008. Endogenous and exogenous control of ecosystem function: N cycling in headwater streams. *Ecology* **89**: 3515–3527. DOI:10.1890/07-1003.1

Walling DE. 1974. Suspended sediment and solute yields from a small catchment prior to urbanization. In *Fluvial processes in instrumented watersheds*, Gregory KJ, Walling DE (eds), Special Publication no. 6. Institute of British Geographers: London, UK; 169–192.

Walling DE, Webb BW. 1987. Suspended load in gravel-bed rivers: UK experience. In *Sediment transport in gravel rivers*, Thorne CR, Bathurst JC, Hey RD (eds). John Wiley & Sons: New York; 691–723.

Wei X. 2003. *Study of the riverine carbon fluxes and erosions in the Zhujiang drainage*, *Dissertation for the Doctoral Degree*. Guangzhou Institute of Geochemistry, Chinese Academy of Sciences (In Chinese): Guangzhou.

Wiegner TN, Tubal RL, MacKenzie RA. 2009. Bioavailability and export of dissolved organic matter from a tropical river during base- and stormflow conditions. *Limnology and Oceanography* **54**: 1233–1242. DOI:10.4319/lo.2009.54.4.1233

Wu Y, Zhang J, Liu SM, Zhang ZF, Yao QZ, Hong GH, Cooper L. 2007. Sources and distribution of carbon within the Yangtze River system. *Estuarine, Coastal and Shelf Science* **71**: 13–25. DOI:10.1016/j.ecss.2006.08.016

Wu Y, Bao H-Y, Unger D, Herbeck LS, Zhu Z-Y, Zhang J, Jennerjahn TC. 2012. Biochemical behavior of organic carbon in a small tropical river and estuary, Hainan, China. *Continental Shelf Research* **57**: DOI:10.1016/j.csr.2012.07.017

Zhang S, Lu XX, Sun HQ, Han JT, Higgitt DL. 2009. Geochemical characteristics and fluxes of organic carbon in a human-disturbed mountainous river (the Luodingjiang River) of the Zhujiang (Pearl River), China. *Science of the Total Environment* **407**: 815–825. DOI:10.1016/j.scitotenv.2008.09.022

Ziegler AD, Bruun TB, Guardiola-Claramonte M, Giambelluca TW, Lawrence D, L NT. 2009. Environmental consequences of the demise in Swidden agriculture in SE Asia: hydrology and geomorphology. *Human Ecology* **37**: 361–373.

Ziegler AD, Sidle RC, Phang VXH, Wood SH. 2014a. Bedload transport in SE Asian streams—uncertainties and implications for reservoir management. *Geomorphology* **227**: 31–48. DOI:10.1016/j.geomorph.2014.01.015

Ziegler AD, Benner SG, Tantasirin C, Wood SH, Sutherland RA, Sidle RC, Jachowski NRA, Lu X, Snidvongs A, Giambelluca TW, Fox JM. 2014b. Turbidity-based sediment monitoring in northern Thailand: hysteresis, variability, and uncertainty. *Journal of Hydrology* **519**: 2020–2039. DOI:10.1016/j.jhydrol.2014.09.010

